31 OCT REC'D

4000

ADVANCE INFORMATION COPY.
FOR RETENTION OR RETURN TO CODE 2628

NRL Report 7785

Preliminary LIBEC/FAMOUS Cruise Results

W. L. Brundage, Jr., and N. Z. Cherkis

Oceanology Area

8000

September 29, 1975

NAVAL RESEARCH LABORATORY
Washington, D.C.

Approved for public release; distribution unlimited.

SECURITY CLASSIFICATION OF THIS PAGE (When Data Entered)

REPORT DOCUMENTATION PAGE		READ INSTRUCTIONS BEFORE COMPLETING FORM
1. REPORT NUMBER NRL Report 7785	2. GOVT ACCESSION NO.	3. RECIPIENT'S CATALOG NUMBER
4. TITLE (and Subtitle) PRELIMINARY LIBEC/FAMOUS CRUISE RESULTS		5. TYPE OF REPORT & PERIOD COVERED Final report on one phase of a continuing NRL Problem 6. PERFORMING ORG. REPORT NUMBER
7. AUTHOR(s) Walter L. Brundage, Jr., and Norman Z. Cherkis		8. CONTRACT OR GRANT NUMBER(s) National Science Foundation Grant AG-264
9. PERFORMING ORGANIZATION NAME AND ADDRESS Naval Research Laboratory Washington, D.C. 20375		10. PROGRAM ELEMENT, PROJECT, TASK AREA & WORK UNIT NUMBERS NRL Problems S01-73.601 (closed) and G05-18
11. CONTROLLING OFFICE NAME AND ADDRESS Department of the Navy Office of Naval Research Arlington, VA 22217		12. REPORT DATE September 29, 1975 13. NUMBER OF PAGES 34
14. MONITORING AGENCY NAME & ADDRESS(if different from Controlling Office)		15. SECURITY CLASS. (of this report) Unclassified 15a. DECLASSIFICATION/DOWNGRADING SCHEDULE

16. DISTRIBUTION STATEMENT (of this Report)
Approved for public release; distribution unlimited.

17. DISTRIBUTION STATEMENT (of the abstract entered in Block 20, if different from Report)

18. SUPPLEMENTARY NOTES

19. KEY WORDS (Continue on reverse side if necessary and identify by block number)

Bottom photography	Lineations
Pillow lava	Scarps
Talus	Fissures
Pelagic sediment	

20. ABSTRACT (Continue on reverse side if necessary and identify by block number)

Analysis of 4882 LIBEC (LIght BEhind Camera) photographs from the Project FAMOUS (French-American Mid-Ocean Undersea Study) median rift valley reveal linear features and bottom surface types. The distribution of the strike of linear fissures and steps on the flat valley floor tends to cluster at N-20°E, the local strike of the valley. The high topography at the valley axis is dominated by thinly sedimented pillow lava on scarp shoulders and by talus on and at the base of steep surfaces.

DD FORM 1 JAN 73 1473 EDITION OF 1 NOV 65 IS OBSOLETE
S/N 0102-014-6601

SECURITY CLASSIFICATION OF THIS PAGE (When Data Entered)

CONTENTS

INTRODUCTION 1

LOCATION AND PHYSIOGRAPHY 1

EQUIPMENT AND METHODS 3

LINEATION TERMINOLOGY 6

STRIKE MEASUREMENT 8

LINEATION TABULATION 8

LINEATION HISTOGRAMS 14

LINEATION CHART 16

BOTTOM CHARACTERISTICS 16

CONCLUSIONS 21

ACKNOWLEDGMENTS 24

REFERENCES 24

APPENDIX A — Lineations 26

PRELIMINARY LIBEC/FAMOUS CRUISE RESULTS

INTRODUCTION

The largest physiographic feature on earth, the undersea mid-ocean ridge system, is cleaved by a discontinuous central depression or rift valley. According to the modern concept of plate tectonics, the rift valley is the zone from which two rigid portions of the earth's crust spread apart. Project FAMOUS (French-American Mid-Ocean Undersea Study) was an international effort aimed at a better understanding of the volcanic and tectonic processes associated with such a spreading center.

This report deals with photographic results from USNS *Mizar* cruise 73-11-10, one of several surveys which preceded the Project's culminating submersible investigations scheduled for the summer of 1974 [1]. During this October 1973 cruise, more than 5000 photographs were obtained with LIBEC (LIght BEhind Camera), a system which permits photography of the ocean floor at greater ranges than were previously possible [2, 3].

Results were first presented to the FAMOUS divers at the Woods Hole Oceanographic Institution in April 1974. Presentation of a lineations map based on unsmoothed navigation and early interpretations prompted a request that this be refined before the final dives to the rift valley. The essential observations, illustrations, and maps were presented at the second LIBEC/FAMOUS data review at NRL on June 13, 1974. A preliminary version of this report [4] was made available to all divers before their departure to the dive site.

LOCATION AND PHYSIOGRAPHY

The primary FAMOUS area of interest was centered at 36°49′N, 33°16′W (Fig. 1), about 340 kilometers southwest of Flores, the westernmost island of the Azores. With the exception of one test lowering made in the vicinity of 36°44′N, 33°16′W all LIBEC photographs were obtained in the darkly stippled area shown in Fig. 1. The location of useful photographic information obtained within that area is along the composite camera tracks illustrated in Fig. 2. The relative magnitude of the navigation error can be estimated from 15 track crossings which have been identified by matching the photographs of a pair of tracks. If there were no navigation error, the matching photographs would be at the same point on the smoothed navigation chart. The smooth navigation chart shows the matched photographs to be located between 0 and 240 m apart with an average separation of 113 m.

The hachured areas delineate physiographic features of interest. The thin dashed lines along tracks represent times of poor navigational control. The bottom characteristics indicated by other track symbols will be discussed later.

The hachured zones along the west and east sides of Fig. 2 outline the respective west and east walls of the median rift. The well-defined closely packed contours of the west wall (inset map, Fig. 2) nicely define its boundaries. These same depth ranges were then used to define the more gently sloping east wall by projecting them laterally. The

Note: Manuscript submitted: June 13, 1975.

local downward slope of the valley floor toward the north can be seen from the 1300-fathom (2377-meter) contour, which migrates from the bottom to the top of the walls in a south-to-north direction. The hachured areas in the center locate Mt. Venus to the north (depths less than 2606 m) and Mt. Pluto to the south (depths less than 2560 m), the prime cites of interest for the diving phase of the Project. The letters and numbers bordering Fig. 2 are the index to a master photomosaic map (scale 1:250) used for the initial data reviews mentioned in the introduction. The scale size of each index square is 250 m.

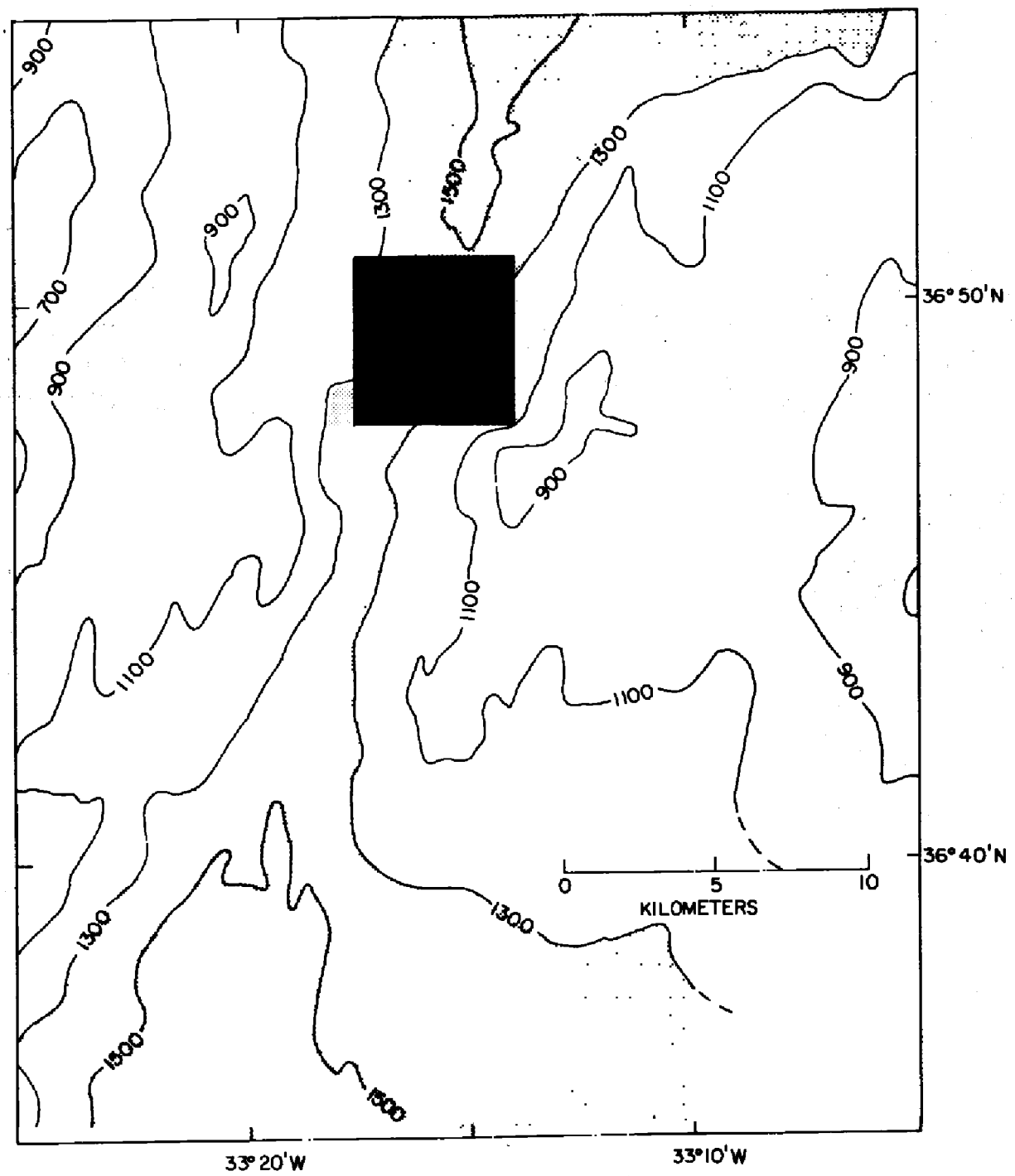

Fig. 1 — Outline (darkly stippled area) of a 5.25-by-5.50-km area in which the LIBEC bottom photographs were obtained as related to the surrounding bathymetry of the mid-Atlantic ridge. The lightly stippled area indicates depths in excess of 1300-fathoms (2377 meters), the contour which locally defines the extent of the median rift valley [5].

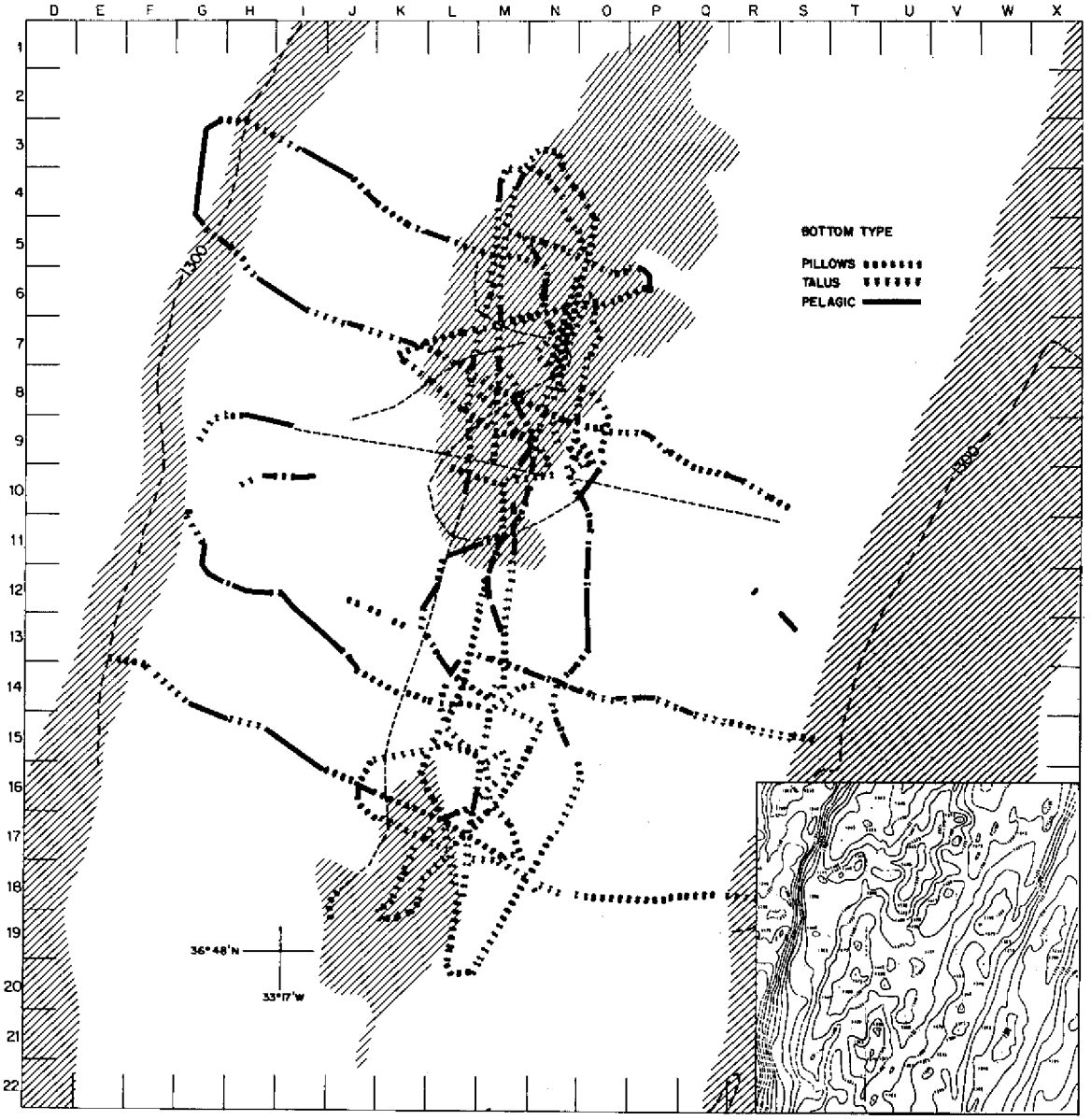

Fig. 2 — Tracks showing the continuous overlapping coverage of LIBEC photographs projected on major features (hachured areas) of local relief in the darkly stippled area of Fig. 1. Track symbols denote the three predominant types of bottom. The inset chart, lower right, is from Ref. 5.

EQUIPMENT AND METHODS

The LIBEC system was deployed through MIZAR's center well and towed by an armored cable which also served as a telemetry link. Figure 3 depicts the submerged portion of the system as it would appear at a bottom-to-camera distance of 10.3 meters. All photographs were taken with a Type 103 Astro Nautical Research 70-mm camera having

a seawater focal length of 40.4 mm. The camera was oriented so that the two straight edges of the picture area were normal to the towing direction. These edges spanned a distance of 57.3 mm, with an angular coverage of 70.6°. The useful crosspath (circular) image spanned about 74 mm or 85°.

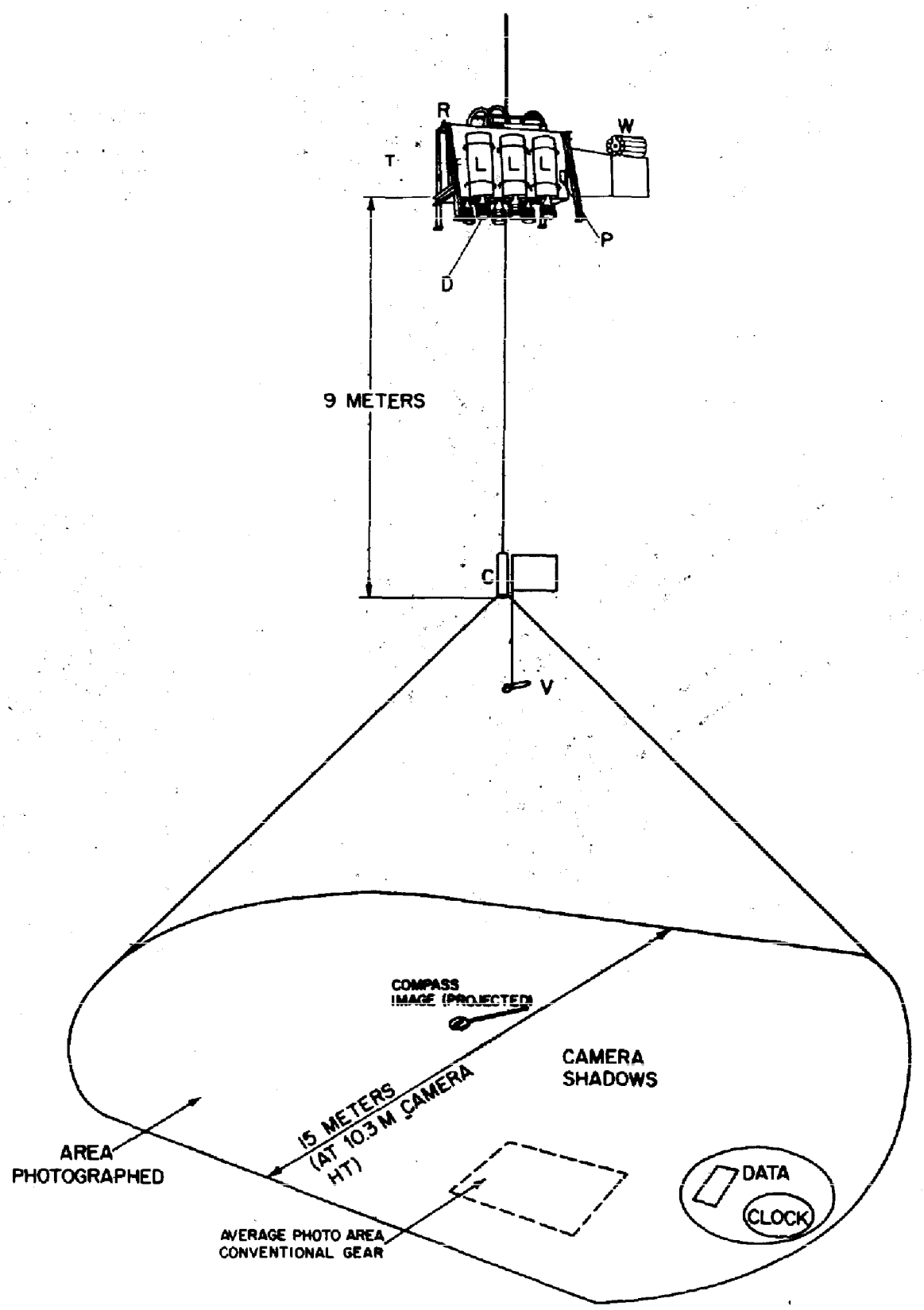

Fig. 3 — Spatial relationship of the deep-towed LIght BEhind Camera (LIBEC) system. Electronic flash lamps (L) provide light which is directed via blackened cones (D) to the outer edges of the field of view of the camera (C). The camera is suspended far beneath the region of intense backscatter that reduces the range at which photographs may be taken (the square represents the average photo taken with normal gear). Other elements in the system during *Mizar* cruise 73-11-10 were a responder (R) for acoustic positioning, a pinger (P) for acoustic altitude, a multiple water sampler (W), an NUS Model 1310 precision temperature sensor (T), and a vaned compass (V) suspended from the camera.

The scale in each photograph can be measured, provided the height is known. The camera height was recorded for camera lowerings (runs) 8 through 14 on a Precision Graphic Recorder by means of acoustic signals. Since the signals originated from a point near the light source, an image of the camera was obtained on the record (Fig. 4).

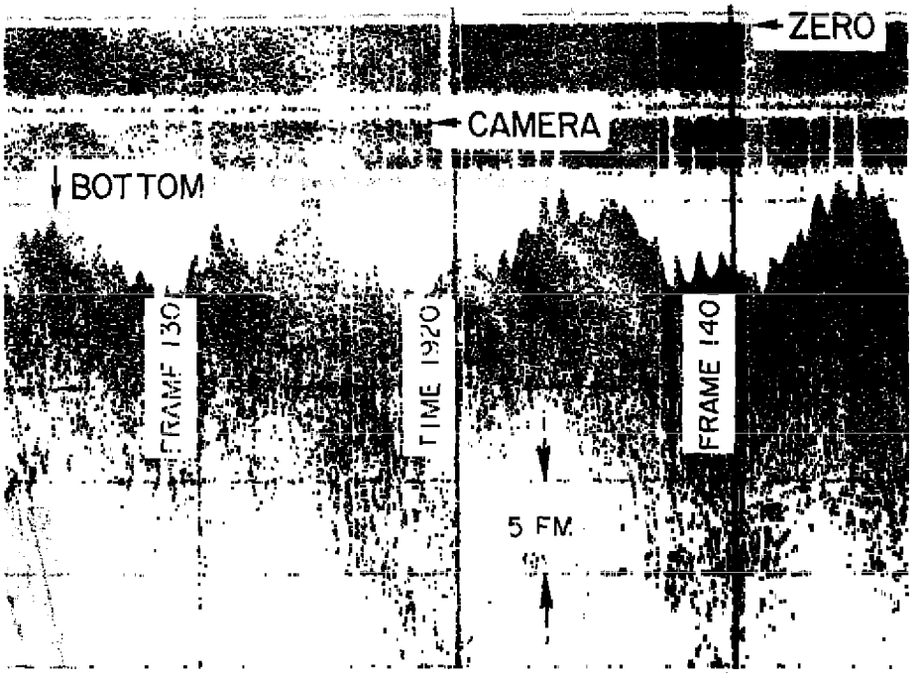

Fig. 4 — Portion of continuously recorded acoustic (pinger) signals from which the camera altitude above the bottom was derived. Small-amplitude changes in the bottom record are artifacts of sea-surface-induced vertical motions of the system.

Interpretation of the LIBEC photographs presents a challenge to those unfamiliar with the geometry of the system. The orientation, relative location, and size of shadows plays a role in determining relative displacement and steepness of surfaces. Figure 5 illustrates graphically how one determines the size and spatial location of an object photographed in midwater. The shadow of the animal is displaced toward the center of the photograph. The same holds true for objects with vertical relief on the sea floor. The concentricity of shadows causes the illusion that surfaces on the periphery of a LIBEC photograph are higher than those toward the center.

The data presented here are based on a study of 4882 readable* photographs (Table 1, camera runs 4 through 6 and 8 through 14). Contact-sized transparancies of each wide-angle photo were studied over a diffuse light source using hand lenses of 5 and 10 power. When viewed from a point well beyond the center of perspective, such wide-angle photographs exhibit a disproportionate magnification of the foreground. This will be particularly bothersome in photographs of features having considerable relief relative to the altitude of the camera. Since proper viewing is not always possible with normal vision, it is best to follow the advice of Kingslake [6] and view the prints with "a magnifying lens having

*Both human error and system malfunctions resulted in occasional photographs or groups of photographs which were too close or too far from the target, blank, or overlapping. All other photographs (approximately 400 per lowering) were considered *readable*.

a focal length approximately equal to the distance of the perspective center from the print." In this study, features of interest were viewed with hand lenses having 1-inch focal lengths (well within the ideal distance of 40.5 mm for these contact-sized prints) followed by an unassisted examination at the "normal" focal distance of 180 mm, thus spanning the ideal viewing distance. The proper viewing distance for the majority of photographs presented in this report (Figs. 6-10 and 14-16) is 63 mm.

Table 1
Summary of LIBEC/FAMOUS Bottom Photography

Run	Oct. 1973 Date	Photography Time (GMT + 1)			Readable Photo-graphs	Remarks
		Start	Finish	Data Gaps		
1	6	0006	0418	0219-0418 (intermittent)	359	Test run to south of study area
2	7	0439	0455	—	4	System malfunction
3	7	—	—	—	—	Camera lost
4	8	1829	2018	Many short gaps	211	Some multiple exposures
5	9	0521	0840	0642-0825	289	Intermittant exposures during gap
6	9	1841	2337	2010-2020, 2156-2326	585	—
7	10	0516	0650	—	4	System malfunction
8	10	1832	2158	—	469	—
9	12-13	1936	0012	—	606	—
10	13	0352	0826	0421-0510, 0524-0559, 0647-0826	448	Latter two gaps intermittant
11	13	1240	1916	1341-1420, 1508-1811	424	Gaps intermittant
12	14	0227	0648	—	615	—
13	14	1235	2259	1255-1845, 2241-2257	621	—
14	15	0252	0712	—	614	—

LINEATION TERMINOLOGY

For this study a lineation was defined as a linelike feature having a length of at least 15 m (the width of a typical LIBEC photograph). Sinuous or irregular features were considered valid lineations if their transverse dimension amounted to no more than a quarter of their visible longitudinal extent. Lineations were divided into five categories illustrated in Figs. 6 through 10 and defined as follows:

scarp (Fig. 6) — A lineation formed by a relatively abrupt change in slope such that a lower surface is not visible due to a lack of light or, if visible, is not flat. Many nonlinear scarps were also noted in the photographs.

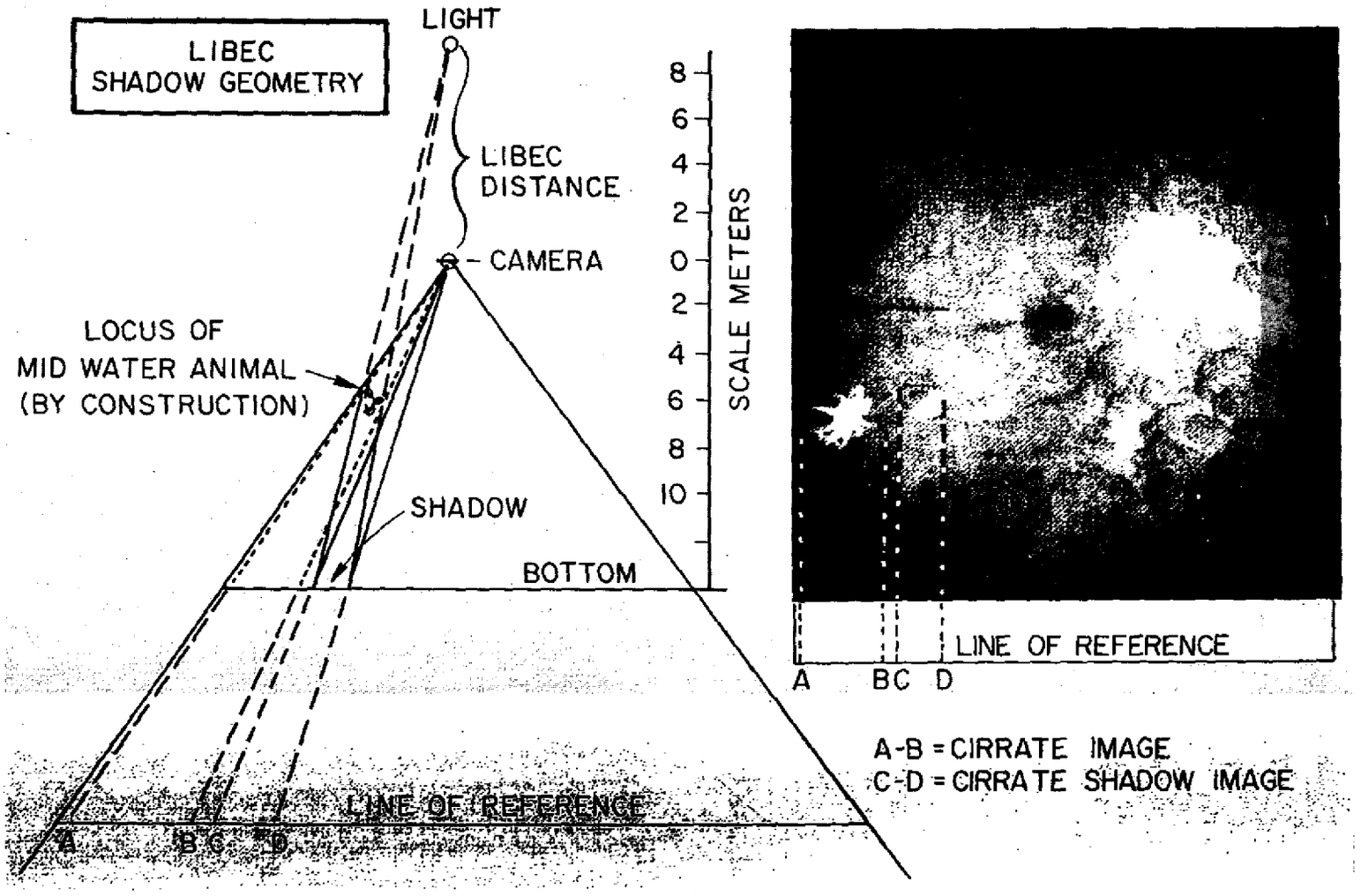

Fig. 5 — Shadow geometry of the LIBEC system. Measurements of an animal (cirrate octopod) and its shadow in the LIBEC photograph at the right are transferred to a vertical plane at the left to graphically reconstruct location and size. The scale was determined by an acoustic record of the altitude.

front (Fig. 7) — A lineation formed by two relatively flat surfaces joined by a third relatively steep surface. The term *fronts* was first chosen to refer to the fronts of lava flows. As the study progressed, it became obvious that some "fronts" were of tectonic origin. The term was retained however to avoid confusion. During a presentation of these results in November 1974 [7] these features were called steps.

fissure (Fig. 8) — A lineation formed by two vertical or almost vertical surfaces with a relatively small opening between. A bottom is usually not visible in the opening.

gully (Fig. 9) — A lineation having two relatively steep sides with a bottom visible between at a vertical distance less than the horizontal separation between the sides. A few fissures were observed to open into (become) gullies in the space of a few photographs. Gullies were therefore later classed as *open fissures* [7].

train (Fig. 10) — A lineation formed by any two or three contrasting bottom-surface types. Several unrelated linear features fell into this category. Many trains were distinguished as a line of pillow lavas denuded of pelagic sediment; these were concluded to mark hairline fissures in which the opening is not discernable and were presented as *closed fissures* in Ref. 7.

STRIKE MEASUREMENT

The horizontal trend or strike of each lineation was measured by aligning the compass image arrow (Fig. 3) with the N-18°W (local-declination) line on a sheet of translucent polar coordinate paper and then noting the true strike of the linear feature in question. Errors were minimized by avoiding measurements on obvious slopes or where a lineation did not cross the middle portion of the photograph. Compass-measured lineations were then plotted by time on the smoothed-camera-track chart using a two-armed protractor with one arm aligned with true north. On photographs having an inoperative or missing compass the lineation strike was measured with respect to the camera vane shadow (Fig. 3) under the assumption that the shadow was aligned with the direction of tow and further that the direction of tow was equivalent to the smoothed-camera-track orientation. These latter lineations were plotted by aligning one arm of the protractor with the smoothed towed-vehicle (fish) track at the time of the observation. The true strike of these relative measurements were then measured with respect to north on the chart. Any near-bottom water movements setting across the camera track would cause the camera vane to assume a drift angle. Any such drift angle is added to errors in track orientation, making these strike measurements much less accurate than those measured directly by compass. Additional errors would also arise because of the several steps involved.

LINEATION TABULATION

Each observed lineation as well as a few other physical features of special significance are tabulated in Appendix A under column headings defined as follows.

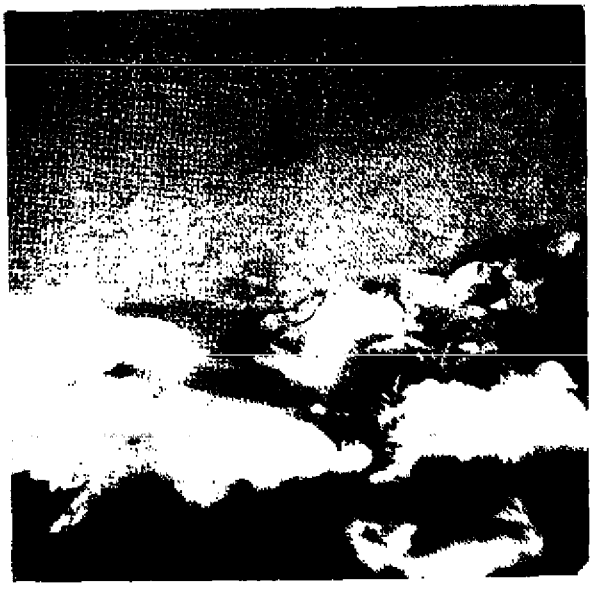

(a) No. 90

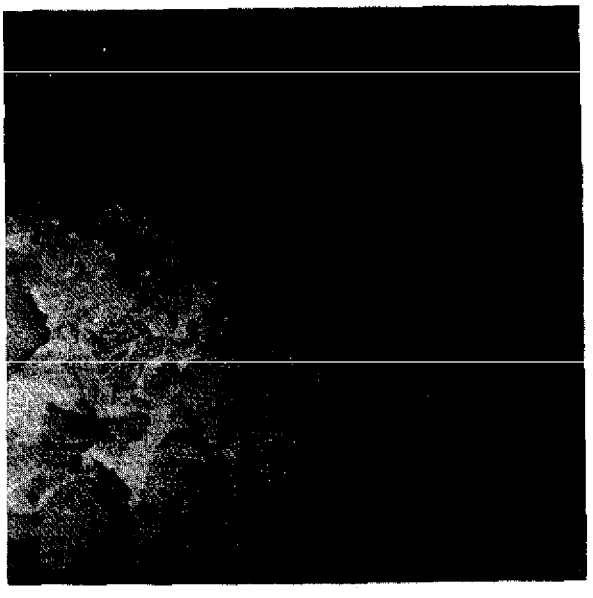

(b) No. 120

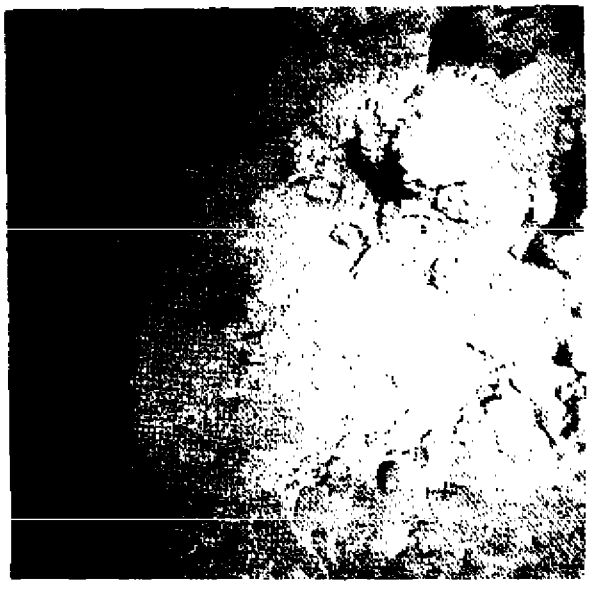

(c) No. 136

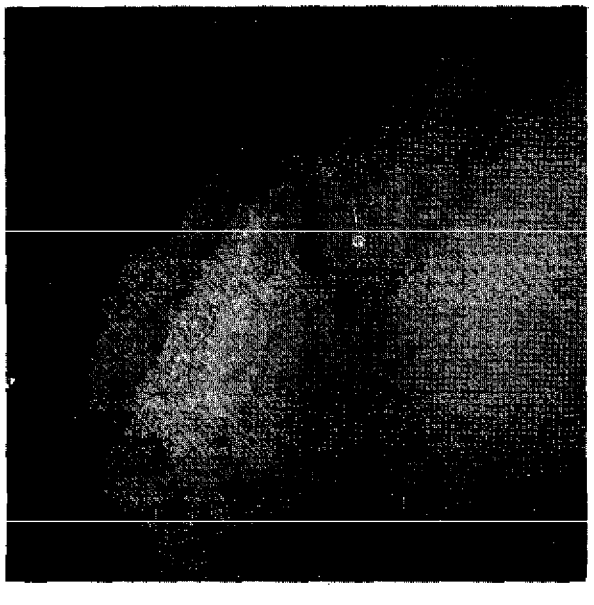

(d) Scarp from run 2

Fig. 6 — Examples of linear scarps (numbered as listed in Appendix A)

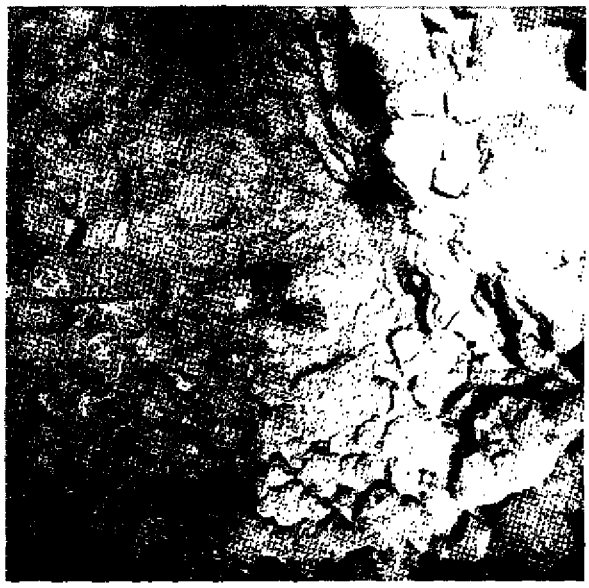

(a) No. 9

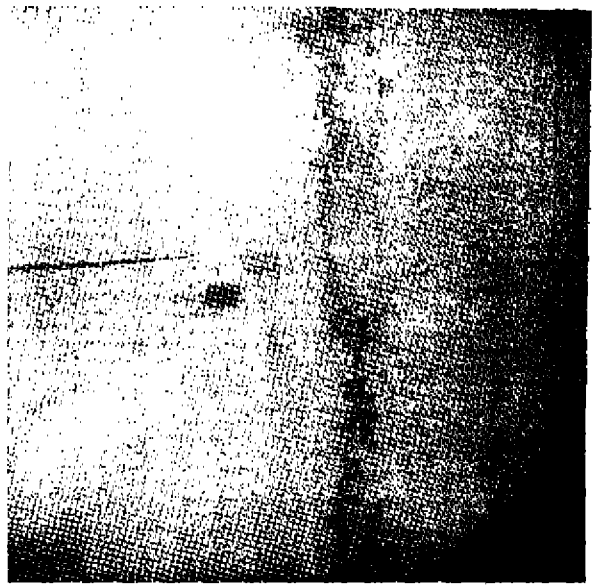

(b) No. 46

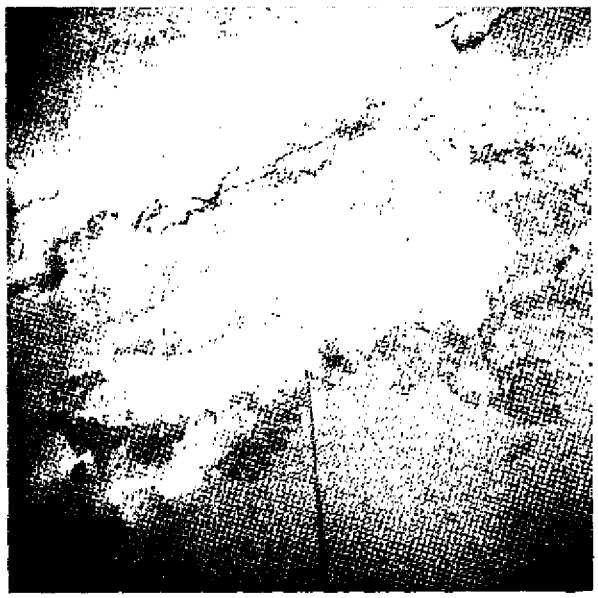

(c) No. 44a

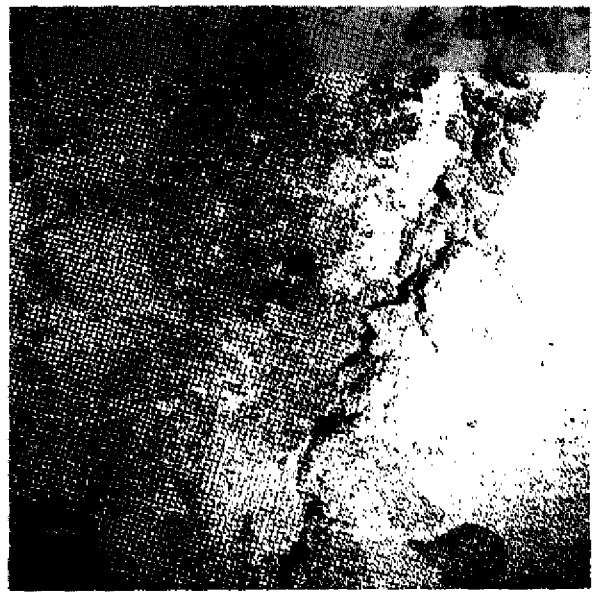

(d) No. 83

Fig. 7 — Examples of linear fronts, or steps

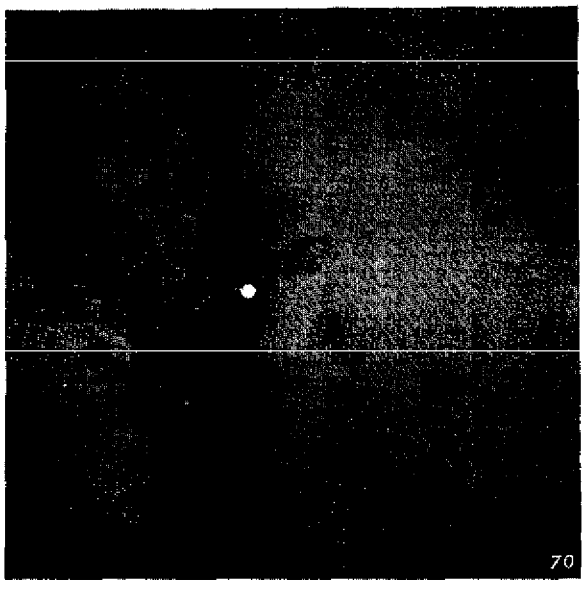

(a) No. 70

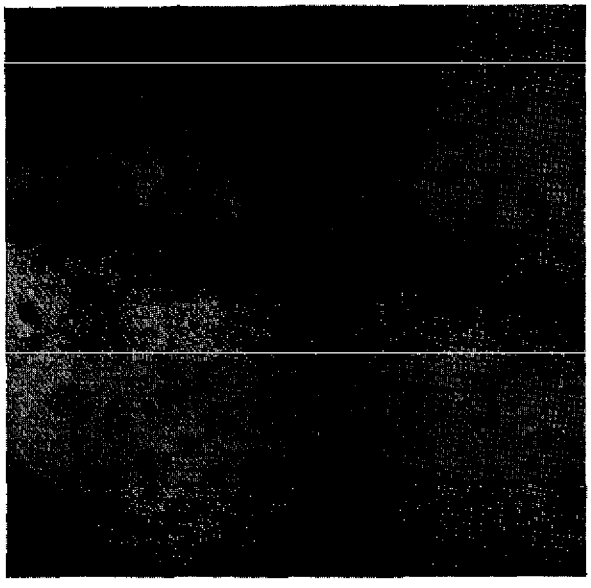

(b) No. 114

(c) No. 167g

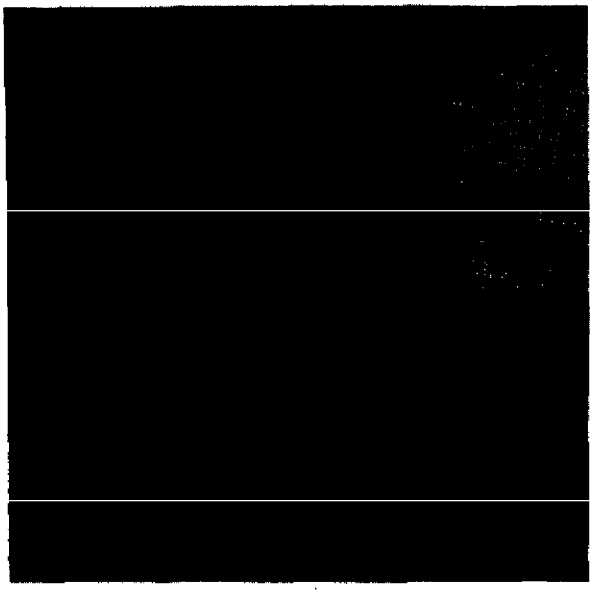

(d) No. 106

Fig. 8 — Examples of fissures

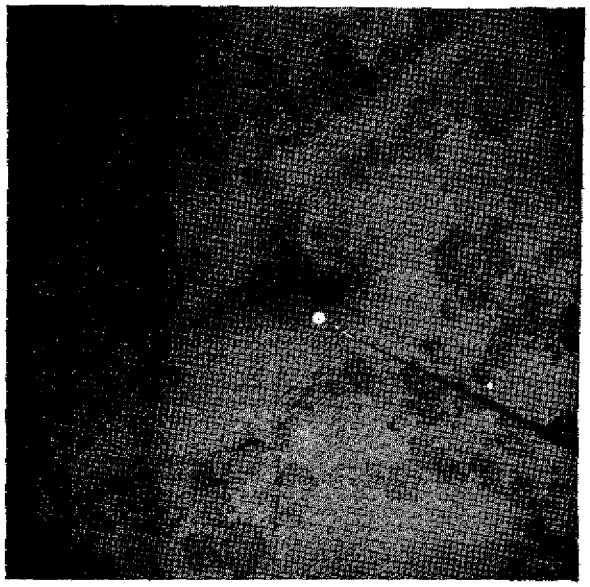

(a) No. 28

(b) No. 18

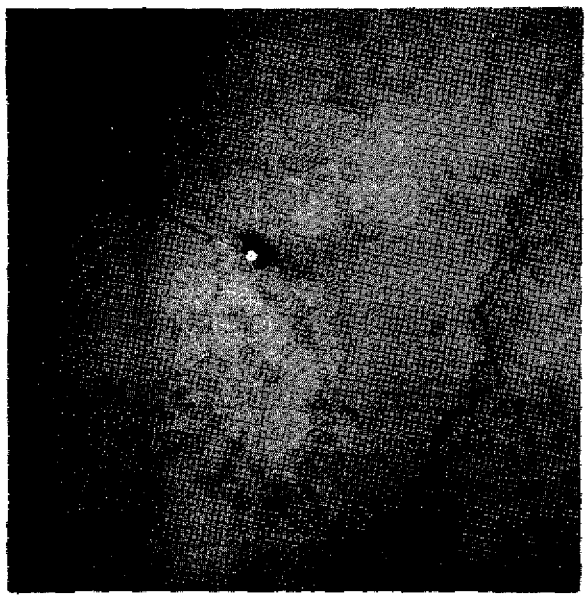

(c) No. 34

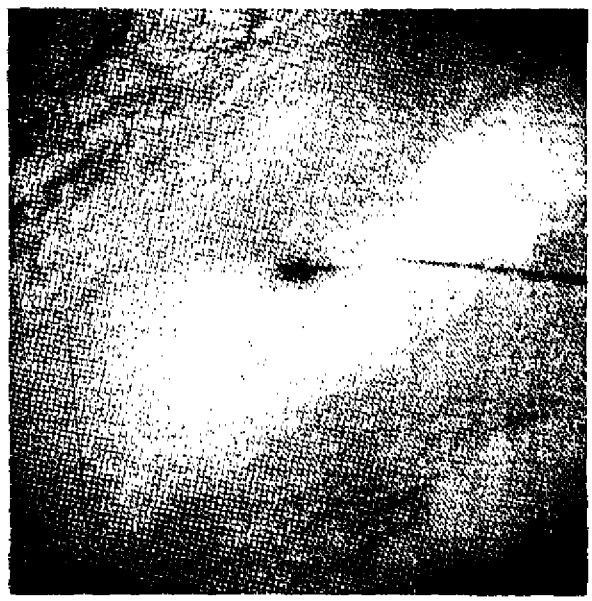

(d) No. 182

Fig. 9 — Examples of gullies, or open fissures

(a) No. 16 (pillows at the upper left to pelagic sediment and dark fines at the right)

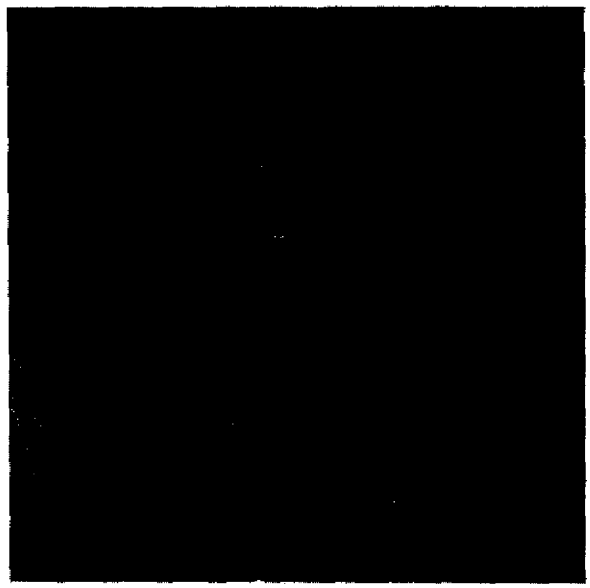

(b) No. 51 (closed fissures)

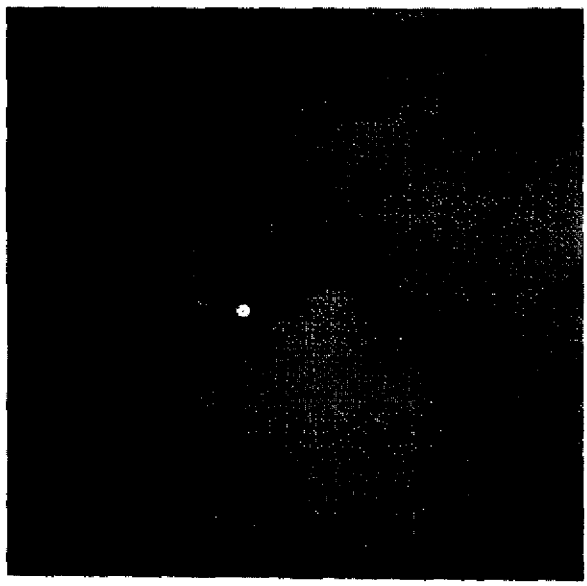

(c) No. 66 (a closed fissure)

(d) No. 77 (a linear swath of dark fines)

Fig. 10 — Examples of trains, a collective term for various linear boundaries between distinct bottom types

No. — The lineation or feature number.

Frame — The number appearing in the data frame at the left (referring to the fish heading) of each LIBEC photograph. The counter is labeled *events.*

Oct. 1973 Date/Time — Day (if it changes) followed by the time (to the nearest minute) as read on the clock in the data frame in each LIBEC photograph.

Type — One of the five nongenetic categories of lineations as defined in the preceding section.

Strike, True — Azimuth of lineation in degrees east or west of true north as measured in photographs in which an operating vaned compass appears. If both this and the subsequent column are filled, the strike was measured after being mapped as noted previously.

Strike, Relative — Azimuth of lineation in degrees to port (P) or starboard (St) of the forward heading of the fish as determined from the camera shadows (Fig. 3).

Est. Max Slope — Estimated maximum slope (0 degrees being horizontal) of the steepest part of each lineation having a discernable vertical relief in four degrees of steepness as follows: $<30°$, 1; $30°$ to $60°$, 2; $>60°$ to $<90°$, 3; vertical or overhanging 4.

Est. Max Relief — Estimated maximum relief (in meters) of any lineation having a discernable vertical relief.

Down Side — True compass direction (N, S, E, W) toward the lower side or dropoff of lineations having obvious relief. When no compass was in the view, the direction is relative to the camera shadow as follows: forward, F; aft, A; to port, P; to starboard, St.

Remarks — Descriptive comments on the character of the lineation or a cross reference if it is illustrated in Figs. 6 through 10. Several prominent nonlinear features (mainly scarps) thought important enough to retain on the list are termed *invalid* under this column.

LINEATIONS HISTOGRAMS

All valid lineations which had a measurable strike (198 lineations) were counted in 5° increments and plotted as a histogram (bottom portion of Fig. 11). A strong mode occurs at N-20°E, the local axial trend of the median rift valley. The two upper histograms of Fig. 11 compare the compass and relative methods of measuring the strike mentioned earlier. The absence of this mode and the wide spread of data evident in the upper histogram compared with the center histogram is assumed to reflect the greater error of the relative method. In Fig. 12 the three histograms compare the strike by *type* of lineation. Only those measurements made by compass were included. *Scarps* exhibit the least consistent trends, since only short segments of these relatively large features were visible in single LIBEC photographs.

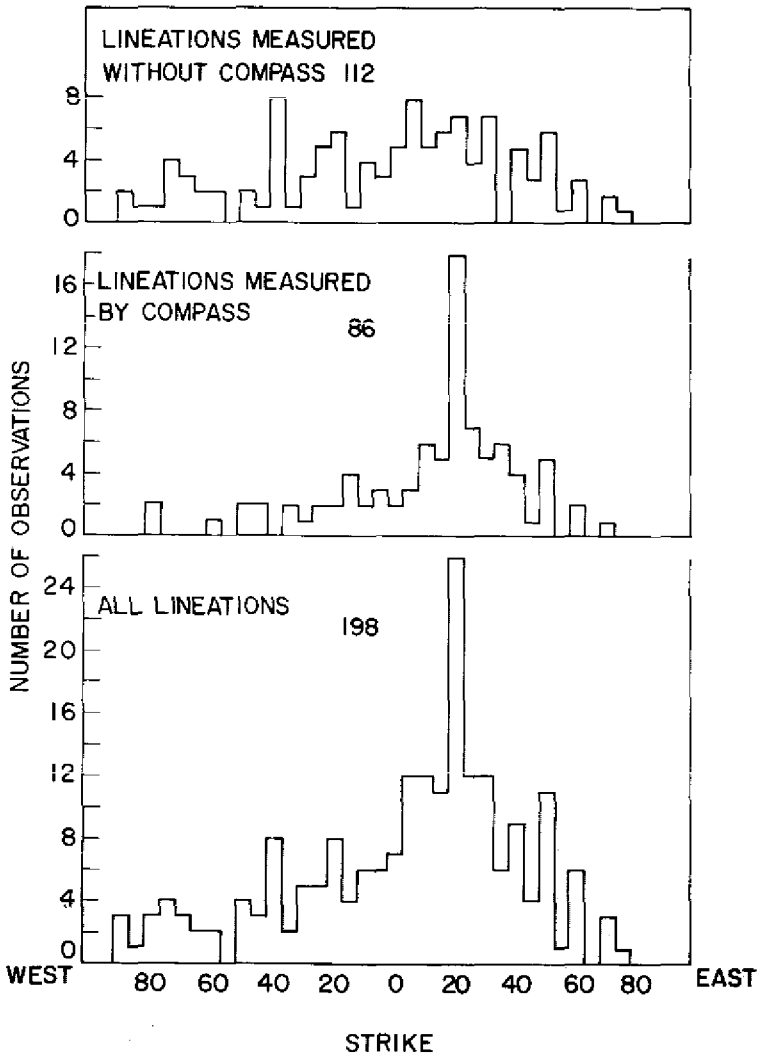

Fig. 11 — A count of lineations versus strike using the suspended compass method (center histogram), the relative method (upper histogram), and both methods added (lower histogram)

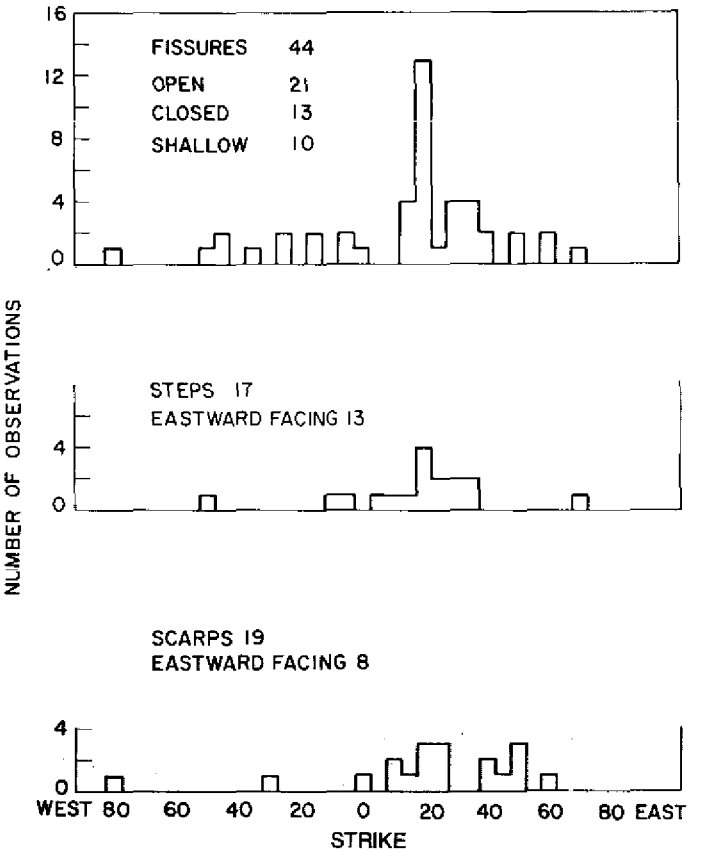

Fig. 12 — A count of lineations versus strike by the compass method comparing different classes of lineations

Both steps (fronts) and fissures exhibit a tendency to cluster about the direction which parallels the main rift valley axis of N-20°E. In the upper histogram, gullies were included as open fissures, and those trains which consisted of linear swaths of pillow lava denuded of pelagic sediment were included as closed fissures. A separate count was made of those scarps and steps which faced easterly. If only those lineations are counted which fall within a 45° arc west or east of north, then slightly less than half (8 out of 19) of the scarps face eastward and 87% (13 out of 15) of the steps face eastward.

LINEATION CHART

Figure 13 is a chart of all valid lineations listed in Appendix A by type with the exception of those which are poorly located (those distinguished by a dagger in the listing). A clustering of scarps is found in the vicinity of the central highs (Mt. Venus and Mt. Pluto). Lineations characterized by less extreme changes in relief appear to be distributed mainly on the relatively level valley floor to either side and between the central highs.

Of the several fissures (lineations 96-98) found on the one camera run which topped the west wall (run 8) two which could be easily distinguished were nearly filled with sediment. Those photographed on the valley floor, on the other hand, were seldom found to have sediment fillings near enough to the top to be illuminated by the LIBEC light source.

BOTTOM CHARACTERISTICS

A first look at the photographs revealed relationships between lineations and gross physical character of the sea floor in the rift-valley study area. Three major bottom types were predominant; these are illustrated in Figs. 14 through 16, charted in Fig. 2, and defined as follows:

pillows (Fig. 14) — Pillow lava rock with its common dark globular shape and surficial cracks is easily recognized. Continuous lava tubes were relatively rare, but some up to 20 m long were noted (Fig. 14c). Collapsed pillows with broken rims (Fig. 14d) were sometimes observed in isolated groups. Pillow lava was usually found in locally flat zones on top of the high topography in the center of the valley.

talus (Fig. 15) — Dark, generally angular rocks in the cobble to boulder size range (Wentworth scale) was mapped as talus. Talus was usually found at the base of scarps and other steep slopes.

pelagics (Fig. 16) —Light-colored surfaces were presumed to be accumulations of pelagic ooze. Pelagic sediment covered more than 50% of the bottom in relatively flat parts of the study area such as to either side of Mts. Venus and Pluto.

The three types of bottom were mapped along each camera track in Fig. 2. The cutoff between types was set at 50%; that is, when more than half the photo area was filled with pillows, talus, or pelagic sediment, the symbol for that particular bottom type is charted. If only one or two photos out of a longer uniform series were found to change in type, these were ignored. Instances in which all three bottom types were present without any single type reaching 50% were rare.

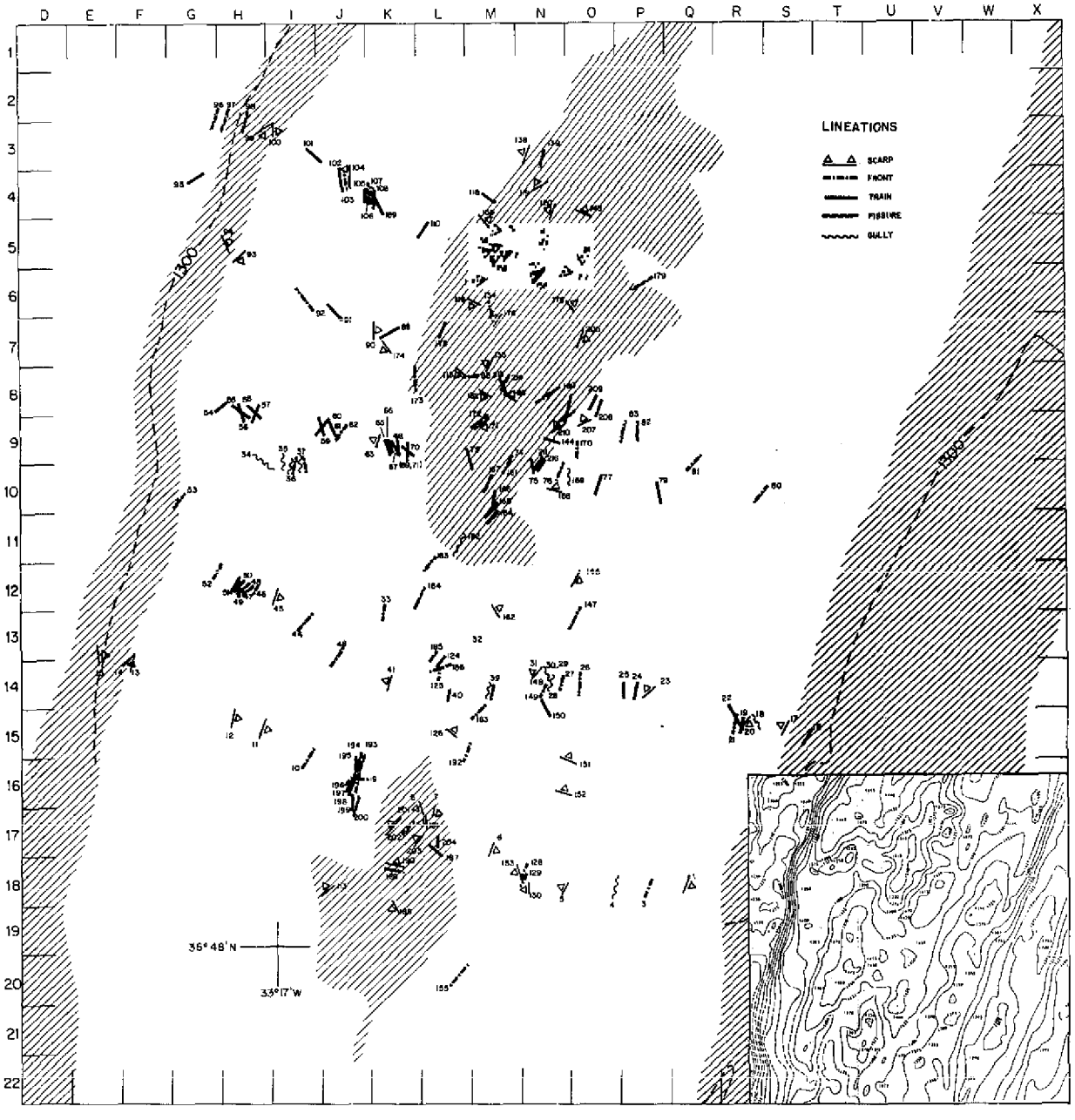

Fig. 13 — Distribution of lineations plotted by type, position, azimuth, and number (Appendix A). Hachured areas are major relief features derived from the detailed bathymetric chart [5] shown in the inset.

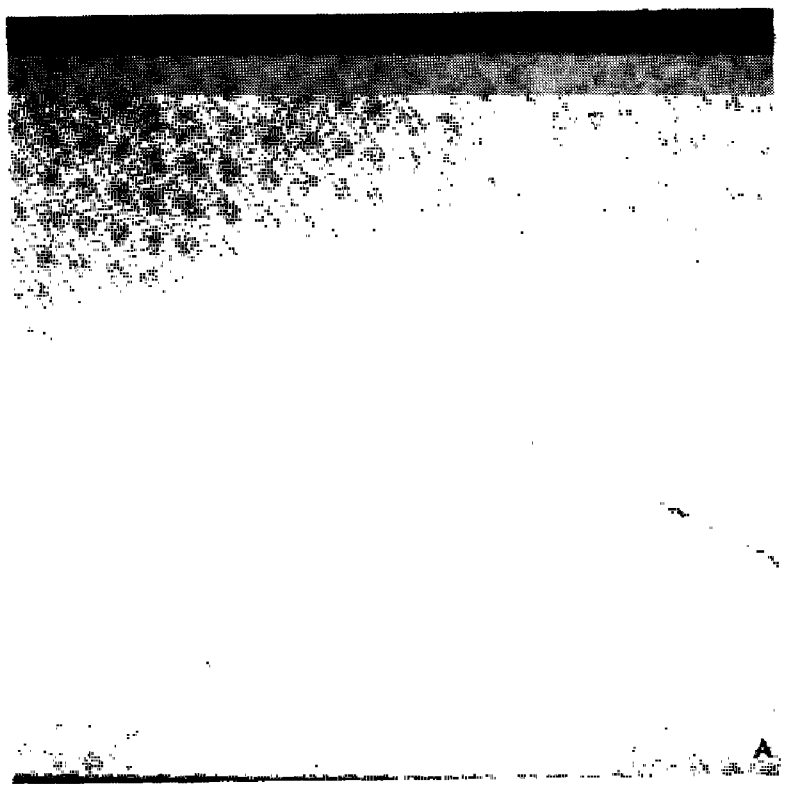

(a) Talus (center) and dark fines (upper left)

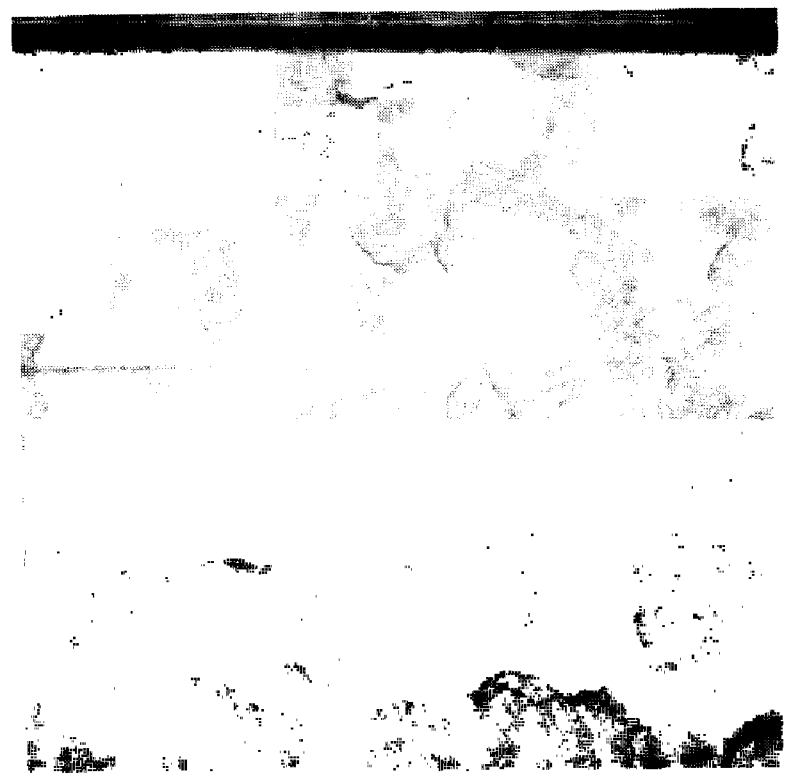

(b) Typical pillow lava

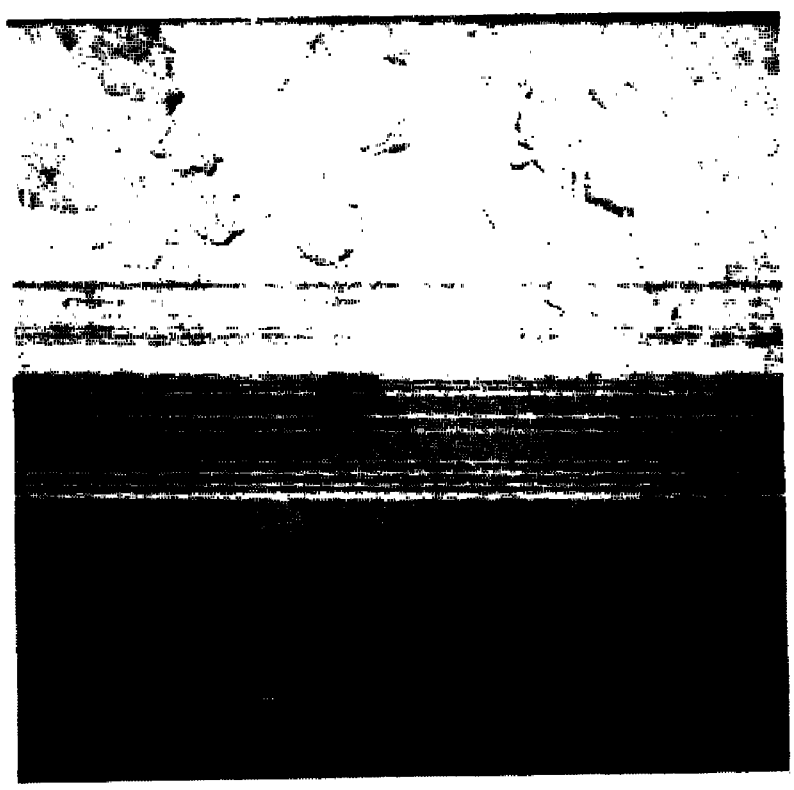

(c) Long continuous lava tube

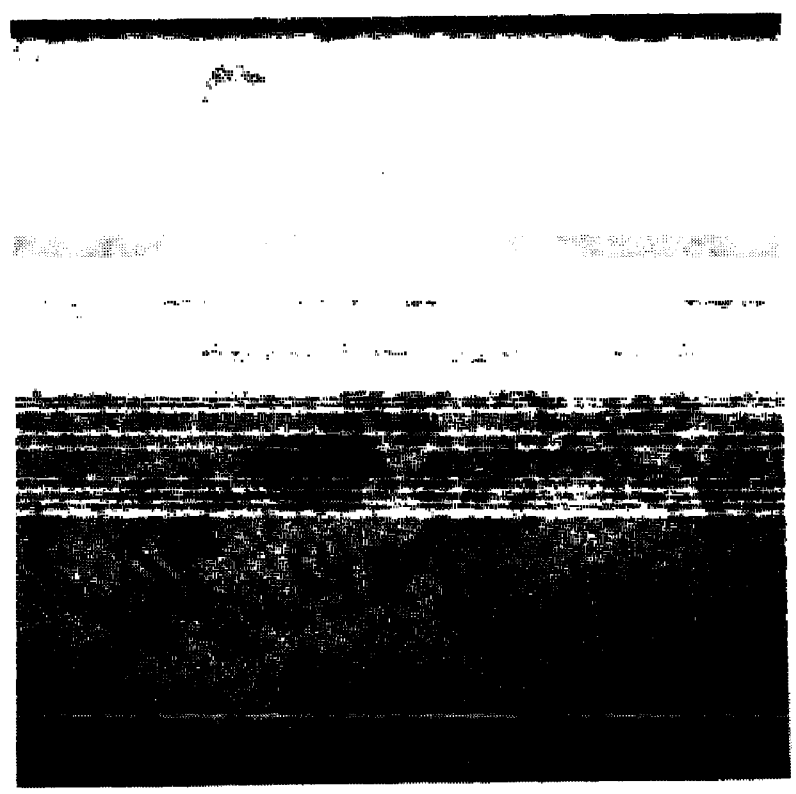

(d) Collapsed pillows with broken rims (upper left)

Fig. 14 — Pillows as distinguished from other dark rocks

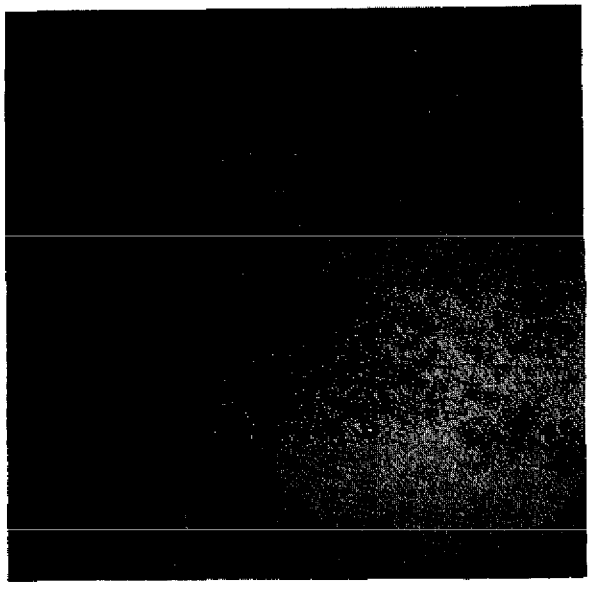

(a) Admixed with pelagic sediment and dark fines

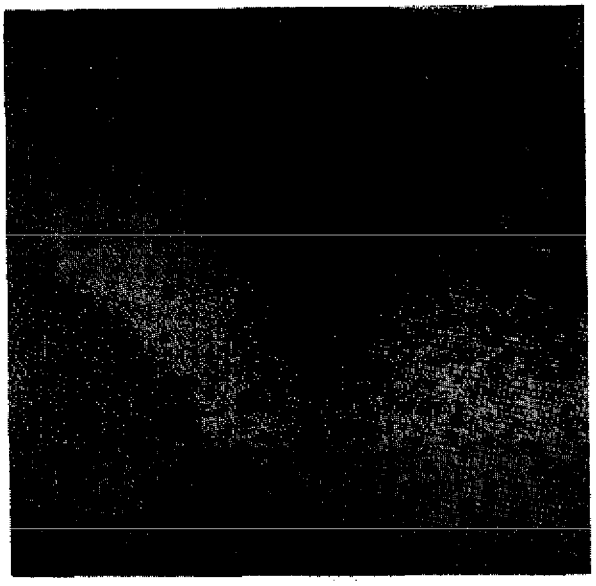

(b) Admixed with a sharply defined tongue of pelagic sediment

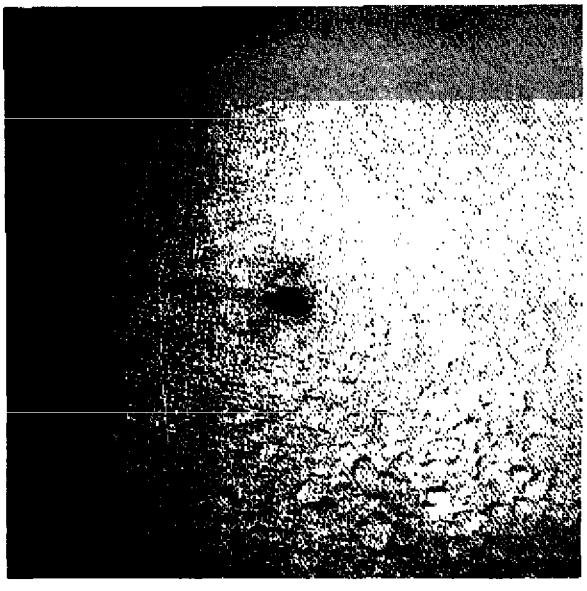

(c) As a uniform cover almost devoid of sediment on the western slopes of Mt. Venus

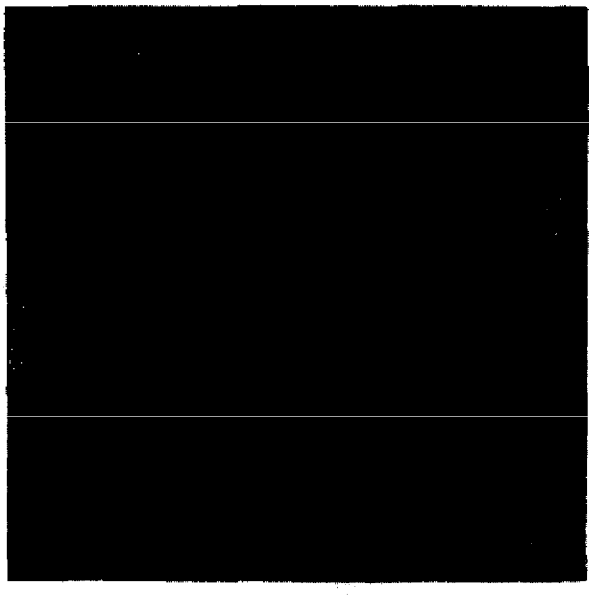

(d) Admixed with sharply defined tongues of pelagic sediment

Fig. 15 — Examples of talus or pillow-lava fragments

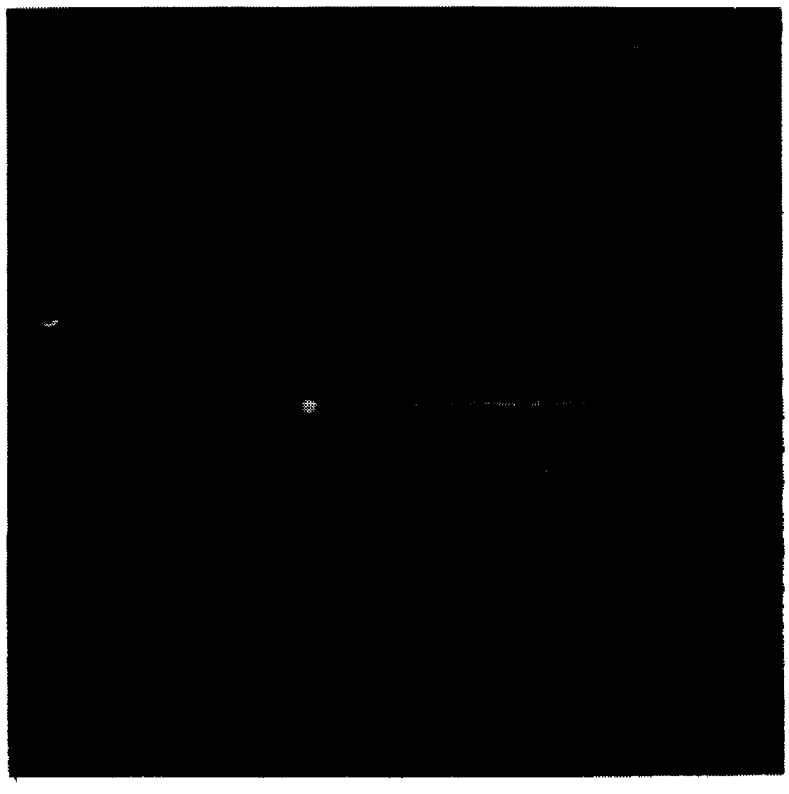

(a) With isolated pillows, including a split hollow pillow (upper center)

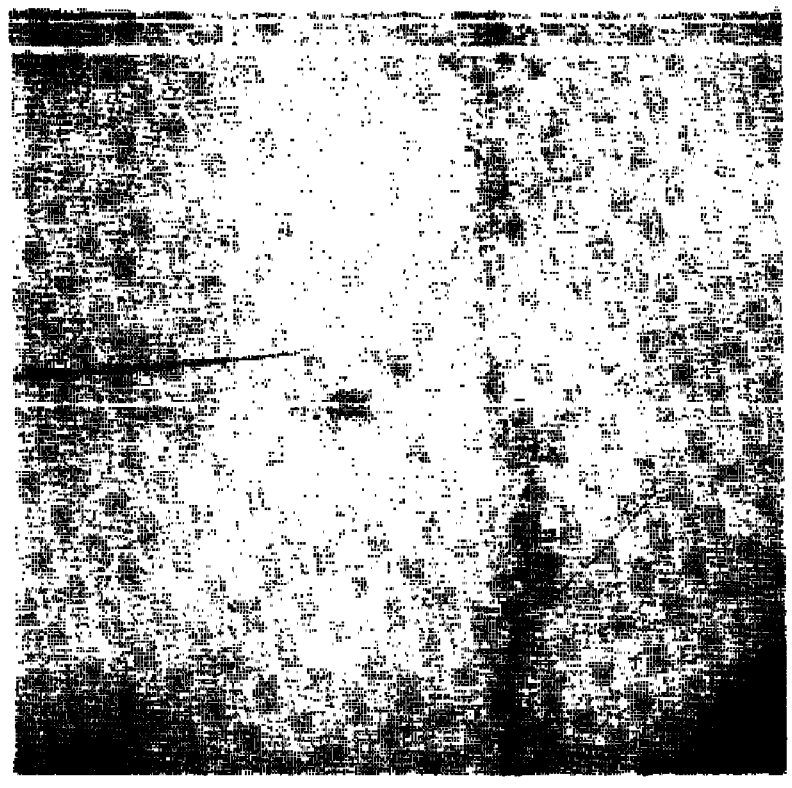

(b) With a closed fissure: lineation 46

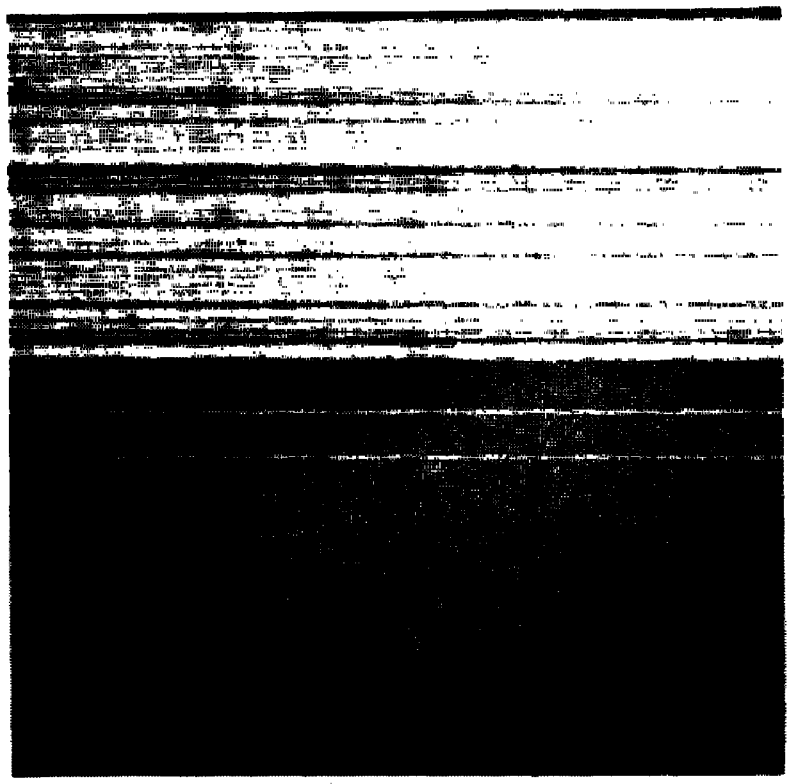

(c) With dark sea urchins and dark fines

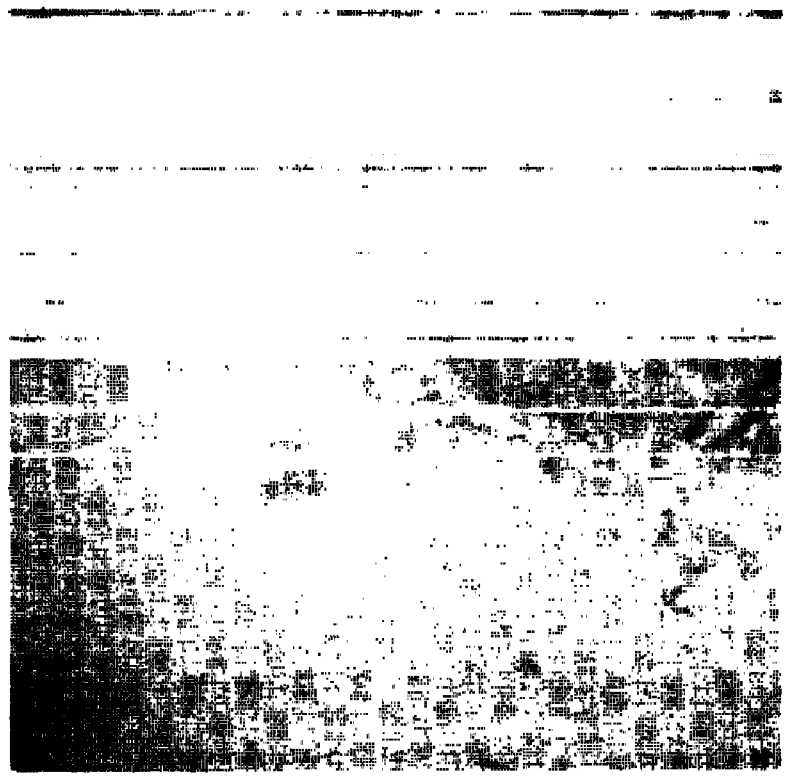

(d) With a sediment-filled circular depression lined with talus.

Fig. 16 — Examples of bottom areas partly covered by pelagic sediment

The central high areas were found to be dominated by pillows and talus with relatively flat parts of the valley to either side and between them characterized by pelagic sediment cover. A notable zone of talus can be seen at and near the base of the west wall as well as a zone of pelagic sediment along the flat area crossed at the top of the west wall on run 8 (upper left in Fig. 2).

A typical boundary between pelagic sediment and pillow lava can be seen in Fig. 17. The portion occupied by pillow lava is toward the right and bottom edges of the mosaic, and a pelagic zone extends out from the center to the left. The upper edge of the montage terminates at lineation 182, a gully or shallow fissure. Talus was most commonly found on the base of steep slopes leading up to scarps.

In some photographs a strip of dark sediment smaller in particle size than talus was noted. One of these can be seen as a vertical swath in Fig. 10d. This sediment is called *dark fines* in this report. Apparently this fine sediment is easily transported, since it was often found to form a current lineation or depositional pattern as in the center of Fig. 9a. In that photograph and in many others the dark fines were seen to occupy a local low in the topography. During run 1, to the south of the study area, dark fines were photographed in a distinct ripplelike pattern. Such features were rarely noted in the photographs from the study area however.

One photograph taken during run 11 near the crest of Mt. Venus exhibits a curious set of dark features believed to be caused by an accidental collision of the towed vehicle with the bottom. The photographic interpretation is shown in Fig. 18. The distance between the scars is equivalent to the distance between the bottom edges of the LIBEC light-source structure (Fig. 3). If the interpretation is correct, then at least locally there appears to be a deposit of dark fine material which is less easily transported than the dark fines previously mentioned. This material apparently fills the interstices between pillows in some areas.

CONCLUSIONS

The following conclusions are limited to features observed in LIBEC photographs and to their relationship with the local bathymetry. More meaningful conclusions await the presentation of other data gathered for Project FAMOUS.

The predominant N-20°E strike of linear features is in close agreement with the strike of the median rift valley, and the eastward-facing attitude of steps (fronts) reflects the overall valley assymetry. It is concluded therefore that the direction of (tectonic) movements which shaped the major valley walls is the same as that which produced the smaller linear features. This conclusion is not valid for those scarps located on Mt. Venus and Mt. Pluto. Because of their close alignment with local isobaths, these scarps are concluded to be a more detailed expression of the shape of the local bathymetry as revealed (and smoothed) by the sonic measurements.

Fig. 17 — A photographically matched crossing between runs 9 and 13

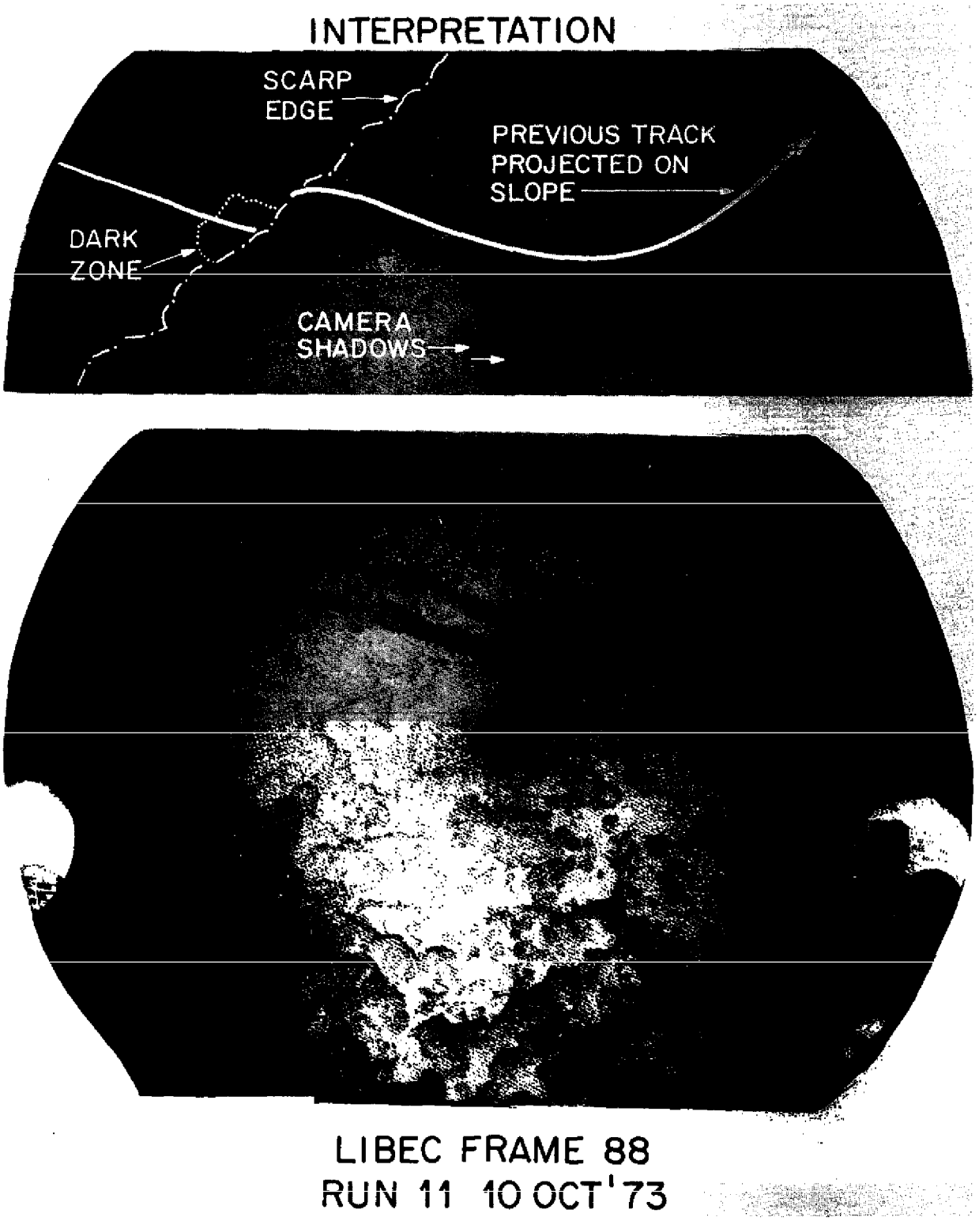

Fig. 18 — Dark markings at the top of a scarp which were probably made by the LIBEC instrument housing on a previous run as shown at the top in the repeated print with interpretation

The distribution of bottom types appears related to the major bathymetry, with pillow lava mantling the upper surfaces of the central highs, talus located along the basal slopes, and pelagic sediment covering much of the relatively low and flat areas between.

The relatively clean rock surfaces noted at the edges of fissures (Fig. 8) suggest that seismic activity detected in the area [8, 9] may reach intensities high enough to help resuspend pelagic sediment. Obviously such edges are free to move at greater amplitudes than the surrounding substrate, and the immediate presence of a sediment trap (the fissure) aids in keeping the surfaces clean. The usual other redistributing mechanisms (by currents and fauna) doubtlessly play a part in the process, but the relative importance of each is unknown.

Mapping by means of strips of overlapping LIBEC photographs is valuable for showing the relationships of bottom-type distributions and features that are too large to be observed by conventional photography or by submersibles and yet are too small to be accurately mapped by surface sonar.

ACKNOWLEDGMENTS

To C.L. Buchanan, senior scientist, and V.A. Del Grosso and E.C. Czul, data acquisition team leaders, and to the officers and crew of USNS *Mizar*, we are extremely grateful. For the use of the data, for helpful guidance, and for a constructive critique of the manuscript we are indebted to H.S. Fleming, senior analyst. For his helpful discussions and smoothing of the navigation data we thank J.D. Phillips, cooperating scientist from Woods Hole Oceanographic Institution. J. Cathro and L. De Marr are thanked for their expert handling of the on-board photographic processing. For the long hours flying the fish and for keeping all systems operational we thank N. Boan, J.P. Campbell, E.W. Carey, Jr., L.L. Cunningham, R.A. Gallatin, H. Gibbs, R.G. Hughes, D.A. Milburn, and R.B. Patterson. For the shore-based photographic assistance we acknowledge R.K. Sibley and his team of experts: in particular J. Cathro, R. Pillard, J. Goff, G. Baker, and W. Farrell. We acknowledge J.M. Brozena, Jr., for his assistance in mapping the lineations and bottom type. Grateful thanks are extended to S.B. Lasher for her efficient typing of the manuscript. Finally we thank R.R. Goodman, Associate Director of NRL, for his inspiration and encouragement before, during, and after the cruise.

The cruise was funded in part through National Science Foundation Grant AG 264.

REFERENCES

1. J.R. Heirtzler, "Project FAMOUS Planning Mid-Atlantic Ridge Investigation," Marine Technology Society J. 7 (No. 1), 14 (Jan.-Feb. 1973).
2. R.B. Patterson, "Increased Ranges for Conventional Underwater Cameras," pp. 153-161 in *Proceedings Underwater Photo-Optical Instrumentation Applications Seminar, Honolulu, Hawaii, March*, 1971, Redondo Beach, Calif., Society of Photo-Optical Instrumentation Engineers, 1972.
3. R.B. Patterson, "Backscatter Reduction for Artificially Illuminated In-Water Camera Systems", Optical Engineering 14, No. 6 (Nov.-Dec. 1975).

4. W.L. Brundage et al., "Preliminary NRL LIBEC/FAMOUS Lineations Report," unpublished manuscript, June 1974.

5. J.G. Moore et al., "Preliminary Model for Extrusion and Rifting at the Axis of the Mid-Atlantic Ridge, 36°48′ North," Geology 2 (No. 9), 437-440 (1974).

6. R. Kingslake, *Lenses in Photography; the Practical Guide to Optics for Photographers*, revised edition, New York, Barnes, 1963, p. 4.

7. W.L. Brundage et al., "Large-Scale Photographs from the Rift Valley in the Project FAMOUS Area," Proceedings of the Geological Society of America, Abstracts with Programs, 6 (No. 6), 671 (Oct. 1974).

8. I. Reid and K. Macdonald, "Microearthquake Study of the Mid-Atlantic Ridge near 37°N, using Sonobuoys," Nature 246, 88-90 (1973).

9. R.C. Spindel et al., "Microearthquake Survey of Median Valley of the Mid-Atlantic Ridge at 36°30′N," Nature 248, 577-579 (1974).

APPENDIX A
LINEATIONS (The section "Lineation Tabulation" defines the headings)

No.	Frame	Oct. 1973 Date/Time	Type	Strike		Est. Max Slope	Est. Max Relief	Down Side	Remarks
				True	Relative				
Run 4 (NRL LIBEC lowering number)									
1	42-43	8/1839	Scarp	15°E	–	3	–	E	–
2	50-53	1840-1841	Gullies	Irreg.	–	3	2	–	Invalid
3	58	1844	Front	20°E	–	4	20	E	–
4	70-71	1848	Gully	35°E	–	2	40	–	–
5	82	1852	Scarp	50°E	–	4	–	W	–
6	140	1911	Scarp	10°E	–	2	–	E	–
7	166-167	1920	Scarp	10°E	–	4	–	E	Very ragged edge
8	177-178	1923	Scarp	20°E	–	4	–	W	Ragged edge
9	213	1935	Front	10°E 90°E	–	4	3	SE	Like an inside corner; Fig. 7a
10	244	1945	Front	35°E	–	1	2	E	–
11	265	1952	Scarp	20°E	–	4	25	E	–
12	280	1957	Scarp	10°E	90°	4	30	A	–
13	318-319	2013	Scarp	20°E	90°	3	50	A	Vertical surface smooth
14	320-321	2014	Front	50°E	70°P	4	–	A	–
15	332	2018	Scarp	N-S	80°St	3	–	A	–
Run 5									
16	73-74	9/0520	Trains	25°E	–	–	–	–	Fig. 10a
17	102-103	0530	Scarp	25°E	–	3	–	W	–
18	133-135	0541	Gully	15°W	–	–	≈1-2	–	Fig. 9b
19	139	0543	Front	15°E	–	–	1	E	–
20	140-141	0544	Train	20°W	–	–	–	–	–
21	143-144	0544	Front	5°E	–	–	–	W	–
22	162	0542	Scarp	40°E	–	2	–	SE	–
23	189-190	0601	Scarp	60°E	–	4	–	N	Irregular
24	211-212	0607	Train	5°E	–	–	1	–	–
25	218-219	0609	Train	5°W	–	–	–	–	Dark fines
26	245	0618	Front	5°W	–	2	2	E	–
27	256	0622	Front	20°E	–	2	4	E	–
28	261	0623	Gully	30°E	–	–	1-2	–	Dark fines; Fig. 9a
29	263-264	0624	Train	10°E	–	–	–	–	Dark fines
30	269	0626	Gully	15°W	–	–	<1	–	Dark fines
31	272	0627	Scarp	40°E	–	3	25	E	–
32	311-312	0640	Train	10°E	–	–	–	–	Pillow size decreases and sediment increases to west
33	1456	0701	Front	10°E	–	2	3-4	E	–
33a	–	–	Fissure	20°E	–	–	–	–	No data image
34	2611-2613	0831	Gully	50°W	–	–	–	–	Fig. 9c
35	2616	0833	Gully	15°W	–	–	1	–	–
36	2619-2621	0834	Gully to fissure	15°E	–	–	–	–	–
37	2623-2627	0835	Gully and front	10°W	–	–	2	W	Meandering
38	2639	0840	Fissure	N-S	–	–	–	–	–

No.	Frame	Oct. 1973 Date/Time	Type	Strike		Est. Max Slope	Est. Max Relief	Down Side	Remarks
				True	Relative				
				Run 6					
39	917-920	9/1851	Gully	15°E	–	–	–	–	Irregular edge
40	953	1902	Train	20°E	–	–	–	–	–
41	982-983	1912	Scarp	25°E	–	3	–	W	–
42	992-993	1915	–	–	–	–	–	–	Invalid; sediment tongue
43	1008-1009	1920	Fissure	35°E	–	–	–	–	–
44	1028	1926	Fronts	30°E	–	1	3	SE	–
44a	1052-1053	1935	Front	15°W	–	2	10	E	Fig. 7c
45	1072-1074	1942	Scarp	20°E	–	4	>50	E	–
46	1089	1948	Front	25°E	–	2	2-3	E	Fig. 7b
47	1090	1948	Fissure	60°E	–	–	–	–	–
48	1091-1092	1948	Fissure	50°E	–	–	–	–	–
49	1094	1949	Fissure	15°E	–	–	–	–	Nearly closed
50	1095	1949	Fissure	35°E	–	–	–	–	Merges with No. 49
51	1096-1098	1950	Triple train	30°E	–	–	–	–	Fig. 10b (two visible)
52	1111	1955	Front	25°E	–	2	10	E	–
53	1160	2010	Front	30°E	–	3	>30	E	Dark fines and light marks at base
54	1212-1214	2028	Train	50°E	–	–	–	–	–
55	1219	2030	Train	45°W	–	–	–	–	–
56	1220	2030	Train	25°W	–	–	–	–	–
57	1227	2033	Train	20°E	–	–	–	–	–
58	1228	2033	Fissure	45°W	–	–	–	–	–
59*	1255-1256	2043	Trains	30°E	70°P	–	–	–	–
60*	1256-1257	2043	Train	5°E	85°St	–	–	–	–
61*	1262-1263	2045	Train	40°W	40°St	–	–	–	–
62*	1266	2046	Front	30°E	70°P	3	10	A	–
63*	1284-1285	2052	Scarp	20°E	80°P	3	>50	A	–
64*	1287-1288	2053	Fissure	20°W	60°St	–	–	–	–
65*	1288-1289	2053	Train	20°W	60°St	–	–	–	–
66*	1289-1290	2054	Train	N-S	60°St	–	–	–	–
67*	1291-1293	2055	Train	35°W	45°St	–	–	–	Fig. 10c
68*	1291-1292	2055	Train	N-S	80°St	–	–	–	Fig. 10c; ends at No. 67
69*	1292-1293	2055	Fissure	20°W	60°St	–	–	–	–
69a*	1295-1297	2056	Fissure	40°W	40°St	–	–	–	Fig. 8a; Ends at No. 70
70*	1296-1297	2056	Fissure	50°E	80°St	–	–	–	Fig. 8a
71*	1297-1299	2057	Fissures	40°W	40°St	–	–	–	Fig. 8a –
71a*	1299-1301	2058	Train	40°W	40°St	–	–	–	Ends at No. 72
72*	1300-1301	2058	Scarp		30°P to 60°St	2	>50	F	Invalid
73*	1327	2106	Fissure	10°W	70°St	–	–	–	–
74*	1345	2112	Front	20°E	80°P	–	–	–	–
75*	1357	2116	Fissure	5°W	75°St	–	–	–	–
76*	1367-1368	2120	Front	20°E	80°P	–	≈1	A	–
77*	1389	2127	Train	10°E	90°	–	–	–	Dark fines; Fig. 10d
78*	1401-1402	2130	–		Irreg.	–	–	–	Invalid; mound
79*	1405	2132	Train	20°W	60°St	–	–	–	Dark fines
79a	1423	2138	Front	–†	90°	–	–	–	–
79b	1433	2142	Fissure	–†	85°P	–	–	–	–
79c	1459	2150	Scarp	–†	80°St	4	20	A	–
79d	1494	2331	Fissure	–†	80°St	–	–	–	–
79e	1513	2338	Scarp	–†	90°	3	15	A	Irregular

No.	Frame	Oct. 1973 Date/Time	Type	Strike		Est. Max Slope	Est. Max Relief	Down Side	Remarks
				True	Relative				
				Run 8					
80	48-49	10/1834	Front	45°E	70°P	2	–	F	–
81	83	1855	Front	40°E	60°P	–	5	F	Dark fines
82	107	1904	Fissure	10°E	65°St	–	–	–	–
83	115	1907	Front	10°E	80°St	4	5	A	Fig. 7d
84	124-127	1912	Scarp	–	Irreg.	3	–	St	Invalid
84a	135	1916	–	–	–	1	7	A	Invalid; sediment tongue
85	147-158	1921-1925	Scarp	–	Irreg.	3	–	P	Invalid
86	164-166	1929	Scarp	35°W	30°St	4	–	St	–
87	173	1931	Scarp	–	Irreg.	4	–	F	Invalid
88	189	1938	Front	85°W	25°P	2	20	F	–
89	233-234	1957	Trains	70°E	40°P	–	–	–	Pelagic to talus
90	241	2000	Scarp	N-S	70°St	4	>30	A	Fig. 6a
91	251-253	2005	Trains	60°W	10°St	–	–	–	–
92	293	2010	Front	40°W	30°St	2	20	St	–
93	299-301	2025	Scarp	45°E	90°	3	–	A	–
94	308	2028	Scarp	25°W	20°St	4	–	St	–
95	344	2043	Trains	50°E	40°St	–	–	–	–
96	371-372	2055	Fissure	30°E	65°P	4	2	–	Bottom visible; dark sediment
97	374	2056	Fissure	30°E	65°P	4	–	–	Bottom visible, one end
98	378-379	2058	Fissure	20°E	90°	–	–	–	Too high for detail
99	384	2100	Scarp	60°E	60°P	4	–	–	Very complex
100	393	2104	Scarp	10°W	50°St	4	–	–	Irregular
101	428-429	2118	Train	60°W	0°	–	–	–	Dark fines
102	454	2129	Train	5°E	60°St	–	–	–	–
103	455	2130	Front	N-S	50°St	4	5-6	–	–
104	456	2130	Scarp	N-S	50°St	4	–	–	–
105	466-467	2134	Train	5°E	50°St	–	–	–	–
106	468	2135	Fissure	5°E	50°St	4	–	–	Fig. 8d
107	469-470	2135	Fissure	5°E	50°St	4	–	–	–
108	471	2135	Trains	5°E 30°W	50°St 25°St	–	–	–	–
109	482	2141	Scarp	–	Irreg.	4	–	A	Invalid
110	484	2142	Train	30°E	80°P	–	–	–	–
111	509-510	2153	Scarp	80°W	0°	3	–	St	–
112	517	2155	Scarp	20°E	90°	4	–	A	–
				Run 9					
113	15-18	12/1939	Scarp	55°E	20°St	4	–	P	Irregular edge
113a	47	1952	Train	–†	60°St	–	–	–	Pelagic to talus
113b	60	1957	Front and fissure	–† –†	20°St 30°St	1 –	2 –	St –	Big collapse rings (frames 61-67)
113c	73	2002	Front	–†	30°St	3	15	St	–
113d	80	2005	Train	–†	10°P	–	–	–	Abrupt rock-size change
113e	100-104	2017	Scarp	–†	Irreg.	4	–	P	Invalid
113f	133	2029	Fissure	–†	10°P	–	–	–	Meandering
113g	137-139	2030	Scarp	–†	Irreg.	–	–	–	Invalid
113h	146-148	2035	Train	–†	0°	–	–	–	Dark fines; meandering
114	161-165	2041-2043	Fissures	–†	Irreg.	–	–	–	Invalid double fissure; Fig. 8b

No.	Frame	Oct. 1973 Date/Time	Type	Strike		Est. Max Slope	Est. Max Relief	Down Side	Remarks
				True	Relative				
Run 9 (continued)									
115	197	12/2057	Scarp	40°W	50°P	4	–	–	Irregular
116	223	2107	Scarp	65°W	80°P	4	30	A	–
117	229	2110	Scarp	50°E	40°St	2	–	P	–
118	249	2121	Train	45°W	50°P	–	–	–	Pelagic to talus
119	303	2144	Scarp	50°W	90°	2	–	–	–
120	311	2148	Scarp	5°E	40°St	–	–	–	Fig. 6b
121	321-326	2152-2154	Scarp	–	Irreg.	4	–	P	Invalid
122	338-339	2201	Scarp	75°E	60°S	4	–	A-St	–
123	397-405	2229-2233	Scarp	–	Irreg.	4	–	–	Invalid
124	501-505	2314-2315	Train	45°E	10°S	–	–	–	Cobbles and dark fines
125	508-509	2318	Train	45°E	10°S	–	–	–	Cobbles and dark fines
126	511-513	2319	Front	–	Irreg.	–	15	–	–
126a	541-542	2331	Scarp	50°W	0°	4	–	P	–
127	566-569	2342-2343	Scarp	–	Irreg.	–	–	–	Invalid
128	625	13/0006	Front	15°E	40°S	2	5	A-St	–
129	631	0008	Front	20°E	50°S	1	–	A-St	–
130	638	0011	Scarp	5°W	20°S	2	–	St	–
Run 10									
131	69-71	13/0417	Scarp	–	Irreg.	4	–	P	Invalid
132	1803	0521	Scarp	75°W	70°P	4	–	A	–
133	1815-1817	0527	Scarp	15°E	10°St	4	–	P	–
134	1840	0535	Front	10°W	10°P	–	–	–	Pelagic to talus
135	1866	0543	Scarp	20°W	30°P	3	–	St	Irregular edge
136	1878	0548	Scarp	75°W	80°P	4	–	A	Irregular edge; Fig. 6c
137	1883	0550	Scarp	70°E	60°St	4	–	F	Irregular edge
138	1921-1922	0605	Scarp	25°E	40°P	4	–	A-P	–
139	1930	0609	Fissure	15°W	65°St	–	–	–	–
140	1938-1940	0613	Scarp	–	Irreg.	4	–	–	Invalid
141	1954-1955	0619	Scarp	–	Irreg.	3	–	–	Invalid
142	1958-1960	0621	Scarp	–	Irreg.	3	–	–	Invalid
143	1977-1978	0628	Scarp	65°W	45°P	3	–	–	–
144	2041	0653	Train	70°W	50°P	–	–	–	Irregular
145	2089-2090	0712	Front	–	Irreg.	1	–	P	Invalid
146	2094	0714	Scarp	25°E	25°St	3	–	–	Irregular
147	2108	0720	Front	25°E	25°St	1	–	St	Irregular
148	2129-2130	0731	Front	60°E	20°St	1	–	St	Irregular
149	2133	0732	Front	15°E	10°P	2	–	St	–
150	2169	0741	Train	30°W	15°P	–	–	–	Dark fines
151	2213	0754	Scarp	70°W	50°P	4	–	A-P	Irregular edge
152	2232	0802	Scarp	75°W	80°St	3	–	A	–
153	2262	0813	Scarp	30°W	60°P	4	–	F-St	–
154	2298	0825	Scarp	–	Irreg.	4	–	–	Invalid
155	2300	0026	Front	40°E	0°	2	–	P	–

No.	Frame	Oct. 1973 Date/Time	Type	Strike		Est. Max Slope	Est. Max Relief	Down Side	Remarks
				True	Relative				
				Run 11					
156	46	13/1241	Scarp	40°W	20°St	4	–	A	Irregular edge
157	83-84	1257	Fissure	60°W	50°St	–	–	–	–
158	86-88	1259	Scarp	40°E	30°St	3	20	A-St	–
159	141-144	1322	Scarps	–	Irreg.	3	–	F-P	Invalid
160	153-154	1326	Front	50°E	15°St	–	2	P	Irregular
161	233	1349	Train	10°E	25°St	–	–	–	Dark fines
162	281	1406	Scarp	25°W	30°P	3	–	–	Irregular edge
163	334	1427	Front	40°E	30°St	1	–	P	–
163a	351-352	1433	Scarp	–†	35°St	3	–	P	–
163b	377-378	1444	Scarp	–†	0°	2	–	–	Very irregular
163c	399	1453	Scarp	–†	80°St	–	–	–	Very irregular
163d	425-426	1502	Train	–†	40°P	–	–	–	–
163e	498	1813	Scarp	–†	60°St	4	20	A	Irregular
163f	501-502	1814	Scarp	–	Irreg.	4	–	F-P	Invalid
163g	506	1816	Scarp	–†	90°	4	–	A	–
163h	544-546	1829	Scarp	–	Irreg.	4	–	F-P	Invalid
163i	566	1836	Scarp	–	Irreg.	3	–	St	Invalid
163j	609	1854	Train	–†	10°St	–	–	–	–
163k	615	1855	Scarp	–†	60°St	3	–	A	–
164	654	1912	Fissure	40°E	40°St	–	–	–	–
165	655	1912	Train	40°E	40°St	–	–	–	–
166	661	1914	Fissure?	15°E	15°St	–	–	–	–
167	663	1915	Fissure?	25°E	25°St	–	–	–	–
				Run 12					
167a	112	14/0303	Scarp	–†	70°P	4	–	A	–
167b	171-172	0328	Scarp	–†	65°P 25°St	3	–	A-P	Outside corner
167c	198	0339	Fissure	–†	30°P	–	–	–	–
167d	249-256	0400- 0403	Fissures	–†	60°St 70°St 70°St 55°St	–	–	–	–
167e	269-272	0408- 0409	Fissures	–†	90°	–	–	–	–
167f	276-278	0411	Fissures-	–†	55°P 65°P	–	–	–	–
167g	289-291	0417	Fissures	–†	80°P	–	–	–	Fig. 8c
168	0317	0428	Scarp	75°W	50°St	2	–	F	–
169	325-326	0431	Gully	15°E	25°P	2	–	–	–
170	365	0449	Front	5°W	70°St	1	3	F	Very irregular
171	403-404	0504	Scarp	50°E	70°P	3	–	A	Irregular
172	404	0504	Fissure	50°E	70°P	–	–	–	–
173	443	0521	Front	N-S	50°St	1	≈10	A-St	Irregular
174	453	0525	Scarp	40°W	70°St	3	–	A	–
175	487	0539	Train	15°E	60°P	–	–	–	Dark fines
176	521-522	0553	Scarp	30°E	50°P	3	–	A	–
177	524-525	0555	Scarp	–	Irreg.	4	–	P	Invalid
178	554	0607	Scarp	40°W	50°St	3	–	F-P	–
179	582-583	0619	Fissure	65°E	30°St	–	–	–	–

No.	Frame	Oct. 1973 Date/Time	Type	Strike		Est. Max Slope	Est. Max Relief	Down Side	Remarks
				True	Relative				
Run 12 (continued)									
180	622	14/0635	Scarp	30°W	30° St	4	–	A-St	–
181	636	0641	Scarp	20°E	90°	4	–	F	–
Run 13									
182	83-85	14/1853	Gully	40°E	–	3	20	E	West wall high & steep; Fig. 9d
183	108	1900	Front	35°E	–	1	5	E	–
184	116-122	1904-1907	Fissures	20°E	–	–	–	–	Double fissure
185	144-145	1916	Fissure	40°E	–	–	–	–	–
186	149	1918	Front	70°E	–	4	<1	S	–
187	248	1958	Front	50°W	–	2	15	NE	–
188	306	2023	Scarp	30°W	–	3	>30	W	–
189	358	2045	Fissure	80°W	–	3	–	–	–
190	361	2046	Scarp	80°W	–	2	–	N	–
191	382-384	2055-2056	Scarp	N-S	–	3	>30	W	–
192	461-462	2128	Front	20°E	–	3	8	E	–
193	519-520	2152	Fissure	25°E	–	–	–	–	–
194	521-522	2153	Fissures	20°E	–	–	–	–	Triple fissure
195	522-523	2154	Fissure	20°E	–	–	–	–	–
196	526-531	2155-2157	Front	20°E	–	3	7	E	Becomes scarplike
197	535-541	2158	Train	20°E	–	–	–	–	Becomes frontlike (frames 540-541)
198	537	2159	Train	35°W	–	–	–	–	–
199	547-548	2204	Train	5°W	–	–	–	–	–
200	549-552	2205	Fissure	20°E	–	–	–	–	Curves more easterly
201	580	2217	Scarp	45°E	–	2	>20	NW	–
202	583-584	2219	Fissure	35°E	–	–	–	–	–
203	590	2221	Scarp	50°E	–	2	>30	NW	–
204	598	2225	Train	05°E	–	–	–	–	–
Run 14									
205	197-199	15/0405	Scarp	25°E	–	2	>20	E	–
206	235	0422	Train	10°E	–	–	–	–	–
207	238	0423	Train	60°E	–	–	–	–	–
208	305	0450	Fissure	20°E	–	–	–	–	–
209	309	0453	Train	20°E	–	–	–	–	Talus to pelagic
210	359-360	0513	Scarp	50°E	–	2	>15	SW?	–
211	391-394	0530	Fissure	20°E	–	–	–	–	–
212	427-429	0542	Scarp	Irreg.	–	3	>20	E & SE	Invalid
213	441-444	0548	Fissure	20°W	–	–	–	–	Crosses No. 214
214	442-443	0548	Fissure	20°E	–	–	–	–	Crosses No. 213
215	471-473	0613	Scarp	Irreg.	–	2	>20	W NW	Invalid
216	603-605	0655	Fissure	30°E	–	–	–	–	–

*Location unreliable.
†Location very unreliable, thus not charted.